Journal of the Mechanical Behavior of Biomedical Materials 179 (2026) 107421

Contents lists available at ScienceDirect

Journal of the Mechanical Behavior of Biomedical Materials

journal homepage: www.elsevier.com/locate/jmbbm

Composition-dependent mechanical properties and viscoelastic behavior of a 3D-printable polyurethane-acrylate soft denture liner

Sangmin Ham [a], Jinhong Min [b], Jiho Lee [b], Young-Bum Park [a], Hoon Kim [b,*], Jaehan Park [c,**]

[a] Department of Prosthodontics, Yonsei University Dental College, Seoul, Republic of Korea
[b] Department of Research Planning, Graphy R&D Center, Graphy Inc., Seoul, Republic of Korea
[c] Department of Prosthodontics, College of Dentistry, Dankook University, Cheonan, Republic of Korea

ARTICLE INFO

Keywords:
Dental polymers
Soft denture liner
3D-printable polymers
Clinical adaptability

ABSTRACT

The long-term clinical performance of conventional soft denture liners is limited by microbial colonization, poor adhesion, and plasticizer leaching. This study developed a polyurethane–acrylate soft denture liner enabling moldless fabrication through digital photolithography-based 3D printing.

Two urethane-acrylate oligomers with different molecular weights (1K: 12900 g/mol, 2K: 18500 g/mol) were synthesized and mixed in five different ratios to investigate compositional effects on mechanical and viscoelastic behavior.

Increasing the proportion of the 2K oligomer enhanced tensile strength and elongation, with compositions ≥1:1 (GR-C) showing mechanical performance comparable to conventional silicone-based soft liners. Dynamic mechanical analysis showed storage modulus values (0.50–0.65 MPa) within the oral mucosal elastic range (0.37–5.93 MPa), indicating damping capacity. Shore A hardness of all compositions remained within the extra-soft range after 30 days, satisfying ISO 10139-2. Under compressive loading, higher 1K content increased resistance to deformation, while GR-C demonstrated intermediate compressive stress at 10–30% strain. In terms of dimensional accuracy, GR-A and GR-D showed greater deviations than the other groups, with higher deviations along the x- and y-axes compared to the z-axis, and group- and axis-dependent patterns were observed. Optical rheometry revealed that increasing the 2K oligomer content reduced the storage modulus while increasing the loss modulus and loss tangent, indicating enhanced viscous behavior.

Water sorption (13.1–14.9 μg/mm^3) was within previously reported ranges, whereas solubility (12.3–16.2 μg/mm^3) was comparatively higher. Near-surface degree of conversion approached 100% after post-polymerization.

GR-C was selected as the optimized formulation and showed no cytotoxicity in an L929 cell assay. In the printability assessment using a novel digital workflow, GR-C exhibited a root-mean square (RMS) deviation of 0.619 mm.

These results demonstrate that controlled oligomer composition enables tunable tensile, compressive, and viscoelastic properties in 3D-printable polyurethane–acrylate soft denture liners.

1. Introduction

Polymers are used in various dental applications, including impression materials, restorative fillings, scaffolds, and prostheses, because of their favorable biomechanical properties, biocompatibility, and processability (Rokaya et al., 2018; Xu et al., 2017). Soft denture liners made of polymer-based materials are applied to the intaglio surfaces of dentures. They are used for short-term applications to promote mucosal healing, and for long-term use to provide cushioning, distribute occlusal forces, and alleviate discomfort (Chladek et al., 2014; Kawano et al.,

*Hoon Kim and Jaehan Park share responsibility as co-corresponding authors for this manuscript.
* Corresponding author. Department of Research Planning, Graphy R&D Center, Graphy Inc., 6th Floor, 225, Gasan Digital 1-ro, Geumcheon-gu, Seoul, Republic of Korea.
** Corresponding author. Department of Prosthodontics, College of Dentistry, Dankook University, 119, Dandae-ro, Dongnam-gu, Cheonan, Chungcheongnam-do, 3116, Republic of Korea.
E-mail addresses: c12o2cl4@gmail.com (H. Kim), imfunny1106@gmail.com (J. Park).

https://doi.org/10.1016/j.jmbbm.2026.107421
Received 30 December 2025; Received in revised form 20 February 2026; Accepted 28 March 2026
Available online 30 March 2026
1751-6161/© 2026 The Authors. Published by Elsevier Ltd. This is an open access article under the CC BY license (http://creativecommons.org/licenses/by/4.0/).

1994a;Kawano et al., 1994b; Onuma et al., 2021; Sato et al., 2000).

Soft denture liners can be fabricated using either direct or indirect methods. In the direct technique, the material is applied chairside between the denture base and the oral mucosa and polymerized intraorally, allowing it to adapt under functional muscle movement. Some commercially available direct liners are marketed for long-term use. In contrast, the indirect method involves impression taking and laboratory-based polymerization, providing greater control over material processing and polymerization conditions, thereby contributing to more stable physical properties.

However, materials for both direct and indirect methods currently used in soft denture liners have notable limitations. Commercial products are broadly classified into those based on silicone or acrylic resin. Despite their favorable long-term durability, silicone-based liners lack chemical adhesion to the denture base and are susceptible to microbial colonization and color instability. Acrylic resin-based liners are typically hand-mixed from powder and liquid, which may introduce porosity and compromise mechanical integrity. Furthermore, the plasticizer may leach out of the material over time, resulting in discoloration, microbial contamination, and unpleasant odors (Braden et al., 1995; Hashem, 2015; Kreve and Dos Reis, 2019; Shiga et al., 2007; Tanimoto et al., 2009). In addition, since the product must be mixed and applied manually, the outcome may be affected, depending on the clinician's skill, resulting in difficulty achieving standardized results (Yamaga et al., 2015).

To overcome these limitations, researchers have developed new materials for soft denture liners (Chladek et al., 2013; Deng et al., 2021; Kanie et al., 2005, 2008, 2009; Kasuga et al., 2011; Santawisuk et al., 2013; Songsang et al., 2022). Among the recently developed materials, polyurethane materials synthesized via the reaction of diols and diisocyanates have shown promise for biomedical use because of their tunable physical properties and favorable biocompatibility (Charlon et al., 2014; Gonzalez, 1978; Kanie et al., 2009; Mishra et al., 2023; Tzeng et al., 2021; Wienen et al., 2023). In particular, the reaction of hydroxyethyl methacrylate (HEMA) with a suitable diisocyanate produces a urethane acrylate oligomer that chemically bonds to denture base resins. Previous studies have shown that the composition of urethane-acrylate oligomers can be controlled to make them suitable for use as soft denture liners (Kanie et al., 2005; 2008, 2009).

Prior research on urethane-acrylate oligomers has adopted an indirect fabrication method using mold-based approaches (Kanie et al., 2005). However, these processes require multiple steps for mold fabrication and may be limited in cases with pronounced undercuts. By using a tabletop scanner and computer-aided design (CAD) software, clinicians can readily replicate the shape of the impression and design a soft denture liner, which can then be fabricated by 3D printing. The fabricated soft denture liner is polymerized while attached to the denture base by applying a liquid oligomer to the intaglio surface. After polymerization, the liner is finished through a trimming process. This digital workflow enables the fabrication of patient-specific prosthesis bases with improved adaptation to complex anatomical situations, without the need for a conventional mold-based approaches.

In the oral cavity, soft denture liners are exposed to harsh conditions owing to the presence of saliva, the oral microbiome, and masticatory forces. Therefore, adequate intrinsic strength and hardness of the material are essential, and maintaining good dimensional and mechanical stability over time under intraoral conditions is critical. In addition, the dynamic viscoelastic properties of soft denture liners influence their long-term clinical efficacy because they are subjected to repetitive, rapidly applied occlusal forces generated during mastication (Kitagawa et al., 2020). Furthermore, biocompatibility is a fundamental requirement for the long-term use of oral materials.

This study synthesized two types of urethane-acrylate oligomers, formulated experimental relining materials at various ratios, and comprehensively compared their properties with those of commercially available soft denture liners to optimize their formulations for clinical applications. The most promising formulation was assessed for cytotoxicity, and printability to evaluate its suitability as a soft denture liner material. Using this approach, we developed a soft denture liner with long-term durability that can be fabricated into patient-specific forms using 3D printing technology, offering capabilities that are not achievable with conventional materials.

2. Materials and methods

2.1. Materials

α,ω-Dihydroxyl-terminated aliphatic polyols with number-average molecular weights (Mn) of 1000 and 3000 g mol^{-1} were used as soft segment precursors. An aliphatic diisocyanate was employed to synthesize the polyurethane prepolymer (Fig. 1). Isodecyl acrylate (IDA, Green Chemical, Seosan, Korea) and isobornyl acrylate (IBOA, Green Chemical, Seosan, Korea) were incorporated as reactive diluent monomers to tailor the viscosity and crosslink density of the UV-curable system. Phenylbis (2,4,6-trimethylbenzoyl)phosphine oxide (Omnirad 819, IGM Resins, Waldwick, Netherlands) was used as the photoinitiator. Omnirad 819 was mixed with the oligomer to fabricate a photocurable, 3D-printable soft denture liner.

2.2. Synthesis of urethane-acrylate and acrylate oligomers

α,ω-Dihydroxyl-terminated aliphatic polyols were first mixed with an acrylic monomer in a 3 L reaction vessel using an overhead stirrer, and the mixture was heated to 40 °C. Subsequently, aliphatic diisocyanate was premixed with 95% dibutyltin dilaurate (291234-100G, Sigma-Aldrich, St. Louis, USA) in a separate beaker and then added to the polyol/acrylic monomer mixture. The urethane-forming reaction was performed at 40 °C for 2–4.5 h. After completion of the reaction, HEMA (0.4 mol%) was added to the mixture and the temperature was increased to 60 °C to conduct capping reaction for 2 h. The formation of urethane bonds and the disappearance of isocyanate functional groups during the reaction between the diol and diisocyanate, as well as during the capping reaction, were confirmed by Fourier transform infrared (FT-IR) spectroscopy. Spectra were recorded in the range of 450–4000 cm^{-1} with a resolution of 4 cm^{-1} and a total of 16 scans. Based on variations in the molecular weight, viscosity, and reaction time under different synthesis conditions, two urethane-acrylate oligomer candidates incorporating hydrophobic monomers were synthesized (Table 1).

2.3. Preparation, printing, and post-processing of 3D-printable soft denture liner

After completing oligomer synthesis, IDA and Omnirad 819 was mixed to enable light polymerization using a digital light processing (DLP) 3D printer (Uniz Slash 2, Uniz, California, USA). The printer was equipped with a 405 nm LED light source, and each build layer was printed with a thickness of 100 μm.

After printing, all polyurethane-acrylate soft denture liner specimens were ultrasonically cleaned in an ultrasonic cleaner (SH-2240D, SAEHAN Ultrasonic Co., Seoul, South Korea) and immersed in 99.5% isopropyl alcohol (Samchun Chemical, Seoul, South Korea) for 1 min to remove residual uncured resin. The specimens were subsequently post-polymerized using a Tera Harz Cure (THC, Graphy Inc., Seoul, South Korea) under nitrogen for 10 min (5 min on both sides). Specimen conditioning was determined according to the objective of each test. Tensile strength, dimensional accuracy, and degree of conversion were evaluated under dry conditions, whereas viscoelastic and compressive behaviors were assessed after storage in 37 ± 1 °C water bath to simulate intraoral environments.

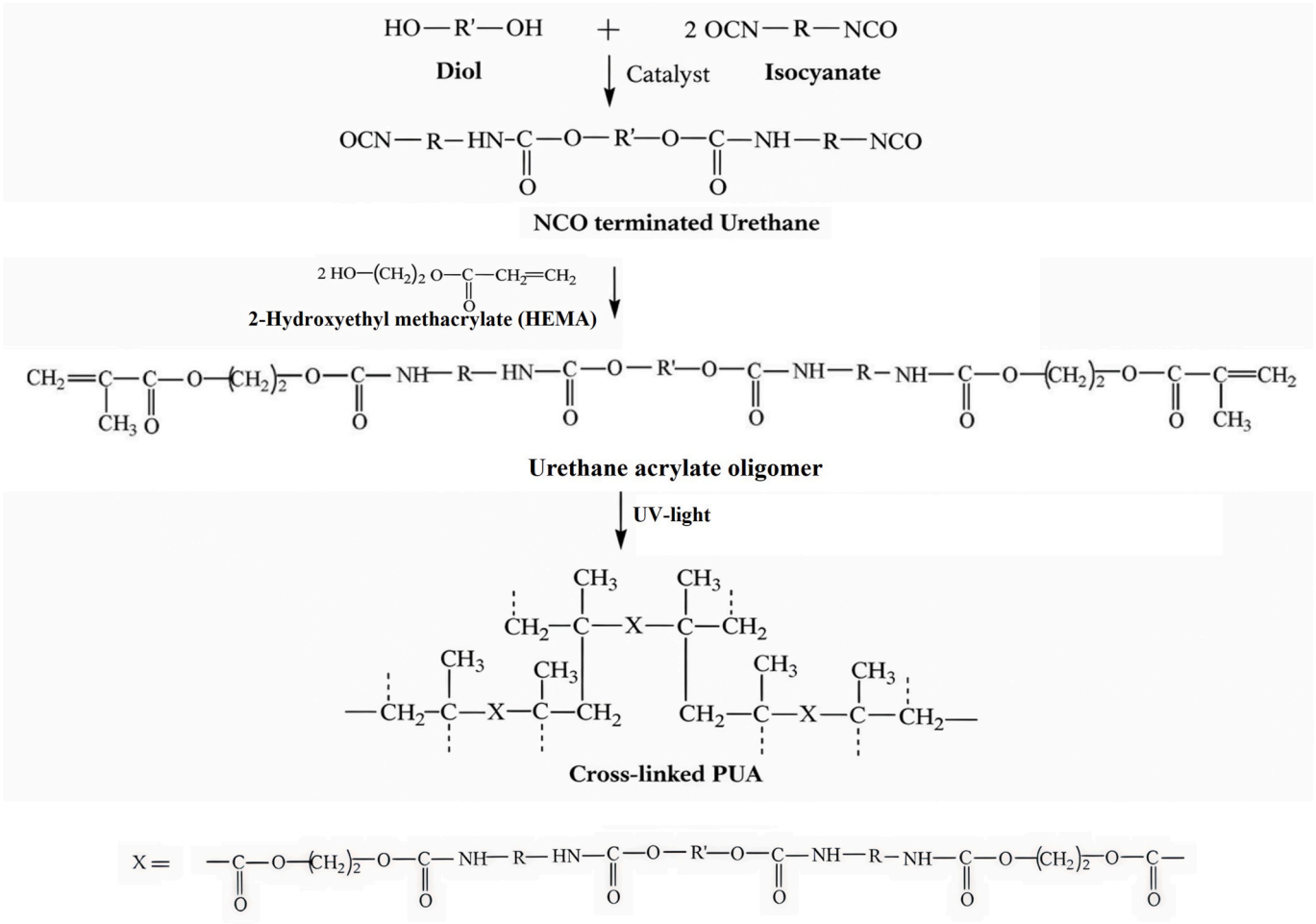

Fig. 1. Schematic of polyurethane–acrylate (PUA) network formation (Maurya et al., 2018). R and R' denote proprietary aliphatic segments.

Table 1
Soft denture liner materials and urethane-acrylate oligomers used in this study.

Commercial Products			
Group	Product Name	Material Type	Manufacturer
CS	Coe-Soft™	Acrylic	GC Corporation
CC	Coe-Comfort™	Acrylic	GC Corporation
RL2	GC RELINE™ II Extra Soft	Silicone	GC Corporation
Synthesized Materials			
Group	Oligomer Ratio (1K: 2K)	Material Type	Manufacturer
GR-A	4 : 0	Polyurethane	Graphy Inc.
GR-B	3 : 1	Polyurethane	Graphy Inc.
GR-C	2 : 2	Polyurethane	Graphy Inc.
GR-D	1 : 3	Polyurethane	Graphy Inc.
GR-E	0 : 4	Polyurethane	Graphy Inc.
Oligomer Characteristics			
Code Name	Molar weight (g/mol)	Viscosity @ 60 °C (cP)	Reaction time (hour)
1K	12900	8350	4~5
2K	18500	18200	7~8

2.4. Comparative evaluation of five different mixing ratios

The physical properties of the polyurethane-acrylate prepared at five different mixing ratios (Table 1) were evaluated. In the tensile strength tests, three commercially available soft denture liners were used as controls: a silicone liner (GC RELINE™ II Extra Soft [RL2], GC Corporation, Tokyo, Japan) and two acrylic-based liners (Coe-Soft™ [CS] and Coe-Comfort™ [CC], GC Corporation, Tokyo, Japan). The specimens were prepared according to the manufacturer's instructions.

2.4.1. Tensile strength and elongation

Seven specimens of each material (RL2, CS, and CC) were fabricated using a conventional molding technique, following the dumbbell-shaped specimen dimensions specified in standard ASTM D638 (overall length: 63.5 mm, thickness: 3.2 mm). For the GR group, the specimens were designed using CAD software, and standard tessellation language (STL) files were exported. Seven specimens were fabricated as described in Section 2.3. Tensile tests were performed using a universal testing machine (Z010, Zwick Roell, Ulm, Germany) at a crosshead speed of 500 mm/min. Stress-strain curves were generated for each specimen, and the ultimate tensile strength and elongation at the point of maximum stress were recorded. Kruskal-Wallis tests and post-hoc analyses with the Bonferroni correction were performed using a statistical software program (IBM SPSS Statistics V28.0, IBM Corp., New York, USA).

2.4.2. Dynamic mechanical analysis (DMA)

Viscoelastic properties are expressed by rheological parameters such as the complex modulus, storage modulus, loss modulus, and loss tangent. The storage modulus (E') represents the elastic component of the material, which enables it to adapt readily to the undercut areas of the oral structures. Also, it is responsible for immediate deformation and recovery in response to occlusal forces. The loss modulus (E'') reflects the

viscous component, allowing the material to dissipate occlusal forces. The magnitude of complex modulus ($|E^*|$) is calculated from the storage and loss modulus and represents the overall resistance of a material to deformation. A higher loss tangent (tanδ) value indicates more viscous and damping-dominant behavior. Each parameter is defined using (Eqs. (1) and (2)):

$$|E^*| = [(E')^2 + (E'')^2]^{1/2} \quad (1)$$

$$\tan\delta = E''/E' \quad (2)$$

DMA was performed using a Q800 system (TA Instruments, Delaware, USA). For each mixing ratio, five cuboidal specimens (30 × 6 × 2 mm) were fabricated using a 3D printer as described in Section 2.3. For comparison, RL2, CC, and CS were used to fabricate cuboidal specimens using a conventional molding technique in accordance with manufacturer's instructions. The first test was performed at a constant temperature of 37 °C, at a frequency of 1 Hz, over a strain range of 0.01–10 % to verify the linear viscoelastic region. The second test was performed at a constant strain amplitude of 1% at the same frequency of 1 Hz over a temperature range of −120 to 60 °C. The rheological parameters were measured under each condition. The glass-transition temperature (T_g) was determined from the peak of the tanδ curve obtained during the second test. The E'' and E' were measured at 36.5 °C, and then tanδ and $|E^*|$ were calculated from these values.

2.4.3. Durometer Shore A hardness tests

A PosiTector SHD Shore Hardness Durometer (DeFelsko Corporation, Ogdensburg, USA) was used to measure Shore A hardness (Fig. 2(a)). The tests were performed in accordance with International Organization for Standardization (ISO) 10139-1:2018 and ISO 10139-2:2016 standards. Using GR series, three cylindrical specimens (diameter of 36 mm; length of 10 mm) were fabricated for each of the five oligomer mixing ratios (a total of 15 specimens), following the same sequence as that used for the tensile-test specimens. Five points at least 1 mm apart were used to measure the hardness of each specimen (Fig. 2 (b)). Testing was performed after storage at 37 ± 1 °C immediately after fabrication and after 1, 7, and 30 days. 3D printed soft denture liners prepared using the five different ratios were classified as soft or extra-soft based on ISO 10139-2:2016. Because the Shore A hardness was repeatedly measured using the same specimens over time, a generalized linear mixed-effects model (GLMM) was applied, with the specimen as a random factor and group and time as fixed effects. An autoregressive [AR (1)] working correlation (clustered by specimen) was fitted to evaluate the effects of group, time, and their interaction on the Shore A hardness. Additionally, Kruskal-Wallis analysis was performed on the mean Shore A hardness values obtained at 1 and 30 days after fabrication.

2.4.4. Optical rheometry

The rheological properties of the resin were assessed using a rotational rheometer (MCR 702e, Anton Paar, Graz, Austria) equipped with a parallel-plate configuration. Oscillatory tests were conducted at 1% strain and 1 Hz. During the test, the specimens were continuously exposed to ultraviolet (UV) light using a UV source (CTLAB ctc4ene4-b63f, 500 W) set to an intensity of 10.3 mW/cm^2 (5% of the maximum output) for 250 s. E'', E', and tanδ were measured for each compositional ratio.

2.4.5. Dimensional accuracy

A cubic model with dimensions of 1 × 1 × 1 mm was designed using CAD software for fabricating specimens (Meshmixer, Autodesk, California, USA). Seven cubic specimens in each group were 3D printed under the same conditions as mentioned in Section 2.3., and the length, width, and height of each specimen were measured using a digital vernier caliper. Deviations from the model dimensions were assessed and subsequently analyzed using a generalized estimating equation (GEE) for the x-, y-, and z-axes, groups, and their interactions. The dependent variable was the deviation, with the specimen specified as the clustering variable to account for within-specimen correlations. A Gaussian distribution with an identity link function was applied, and an exchangeable working correlation structure was assumed for the model.

2.4.6. Compression test

Compression test was performed to evaluate the stress-strain relationship by placing the specimen between two flat compression plates and applying a vertical load. Five cuboid specimens in each group with dimensions of 10 × 10 × 4 mm were designed and fabricated in accordance with ISO 604:2002. Post-processing procedures were identical to those used in the previous tests. Compression was conducted at a crosshead speed of 5 mm/min using a universal testing machine (QM 100TM, Qmesys, Uiwang, Korea). Compressive stress values at predefined strain levels of 10%, 25%, and 30% and the point of failure were reported. A linear mixed-effects model (LMM) was analyzed with group and strain level and their interaction as fixed effects, and specimen as a random effect to account for repeated measurements on the same specimens. Post hoc pairwise comparisons among groups at each strain level were conducted using model-based estimated marginal means with Holm adjustment for multiple comparisons.

2.4.7. Water sorption and solubility test

Disc-shaped specimens (50 × 2.5 ± 0.1 mm) were fabricated. The dimensions of each specimen were measured, and the initial mass (M1) was recorded. The specimens were then immersed in distilled water maintained at 37 ± 1 °C in a thermostatically controlled oven for 7 days. After immersion, the specimens were removed, surface moisture was

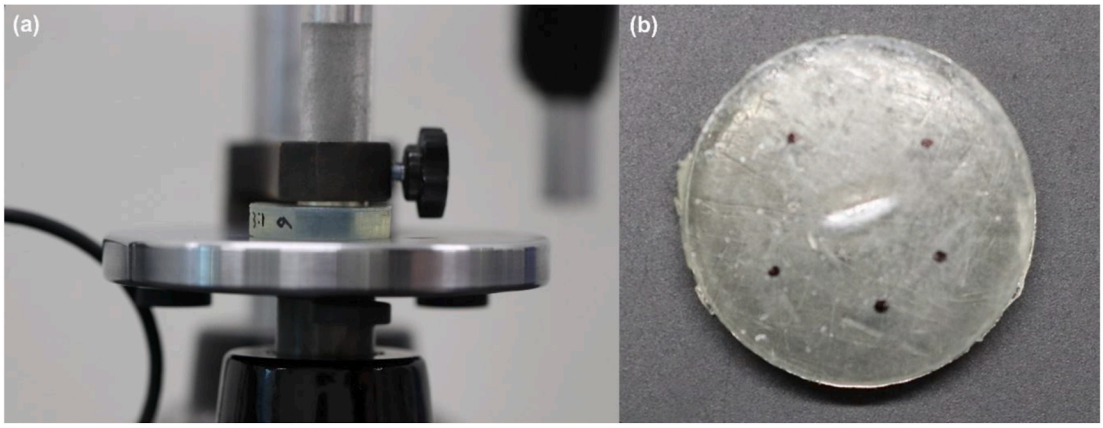

Fig. 2. Shore A hardness test. (a) durometer with specimen in the test setup. (b) cylindrical test specimen.

gently blotted off, and the mass was measured (M2). Subsequently, the specimens were placed in a desiccator containing silica gel and dried at 37 ± 2 °C until a constant mass was achieved, and the final mass (M3) was recorded. Water sorption (WS) and solubility (SL) were calculated according to equations (3) and (4). V denotes the volume of the specimen (mm^3). The results were expressed in $\mu g/mm^3$.

$$WS = (M2 - M3) / V \quad (3)$$

$$SL = (M1 - M3) / V \quad (4)$$

2.4.8. Degree of conversion evaluated by FT-IR

The degree of conversion (DC) of the GR series was evaluated to assess the effectiveness of polymerization after printing and post-processing. DC analysis was performed using FT-IR spectroscopy in attenuated total reflectance (ATR) mode over a spectral range of 450−4000 cm^{-1} with a resolution of 4 cm^{-1} and 16 co-added scans per specimen. The ATR penetration depth was approximately 2.0 μm, and therefore the measured DC values primarily reflect the surface conversion of the specimens. Specimens with dimensions of 10 × 10 × 4 mm, identical to those used in the compression test, were fabricated and subjected to the same printing and post-polymerization procedures described in Section 2.3. Immediately after completion of post-processing, surface conversion was measured.

The percent conversion of the carbon–carbon double bonds (C=C) was calculated based on the relative absorbance ratio of the aliphatic C=C peak at 810 cm^{-1} to the internal reference peak at 1730 cm^{-1}, according to the following equation (5) as described in previous research (Tasic et al., 2004).

$$DC\ (\%) = \{(A_{810} / A_{1730})_a - (A_{810} / A_{1730})_b\} / (A_{810} / A_{1730})_a \quad (5)$$

Where $(A_{810}/A_{1730})_a$ represents the absorbance ratio of the unpolymerized resin and (A810/A1730)b represents the absorbance ratio of the polymerized specimen. If the assumptions of normality and homogeneity of variance were satisfied, one-way ANOVA was performed, followed by Tukey's post hoc test for pairwise comparisons. The significance level was set at 0.05.

2.5. Clinical applicability

After analyzing the effect of the mixing ratio, one formulation from the GR group was selected as the optimal composition for the soft denture liner. The cytotoxicity and printability of the selected group were evaluated to verify their clinical applicability.

2.5.1. Cytotoxicity assessments

The cytotoxicity of the test material was evaluated using both qualitative (microscopic observation) and quantitative (MTT assay) methods in cultured cells. This study was conducted in accordance with ISO 10993-5:2009 guidelines.

An NCTC clone 929 (L929) cell line was purchased from the Korean Cell Line Bank and stored in a −80 °C freezer for 24 h before being stored in liquid nitrogen for long-term storage. The frozen cells were thawed in a water bath at 37 °C. The cells were transferred to Eagle's Minimum Essential Medium (EMEM) with 10% fetal bovine serum (FBS; Gibco, New York, USA) in a centrifuge tube and centrifuged at 1000 rpm for 5 min. The supernatant was discarded. The cells were resuspended in EMEM containing 10% FBS, transferred to a T-75 flask, and cultured at 37 °C in a humidified incubator with 5% CO_2. When the cultures reached approximately 80% confluence, the log-phase cells were detached using 0.25% trypsin–ethylenediaminetetraacetic acid (Gibco, New York, USA), centrifuged, and resuspended in the same medium. Cells were counted using a hemocytometer and adjusted to 1 × 10^5 cells mL^{-1}. Aliquots (100 μL) were dispensed into 96-well plates and incubated for 24 h at 37 °C in a humidified atmosphere of 5% CO_2.

Cubic specimens (with 10 mm sides) were designed in CAD software to have a final mass of 2 g and were fabricated following the same 3D printing procedure as mentioned in Section 2.3. One cubic specimen was immersed in 10 mL of EMEM with 10% FBS and incubated at 37 °C for 24 h. After incubation, the supernatant was collected and designated as the 100% extract. The 100% extract was serially diluted with EMEM culture medium to obtain four two-fold concentrations (50%, 25%, 12.5%, and 6.25%). The negative control specimen was EMEM with 10% FBS and the positive control specimens were aqueous solutions of dimethyl sulfoxide (DMSO; Merck, Darmstadt, Germany) at concentrations of 3%, 6%, and 12%. After the pre-incubation period, the medium of the well plate was removed. Three wells were assigned to each group, and 100 μL of the corresponding negative control, test, or positive control solution was added to each well. The plates were incubated for 24 h at 37 °C in a humidified atmosphere of 5% CO_2. After incubation, the cells were examined microscopically to assess their cytotoxic reactivity. Then, 20 μL of 3-[4,5-dimethylthiazol-2-yl]-2,5-diphenyltetrazolium bromide (MTT, 5 mg mL^{-1} in D-PBS) was added to each well, and the plates were incubated for an additional 4 h. The medium was discarded, and the plates were air-dried. Subsequently, 100 μL of DMSO was added to each well to solubilize the formazan, Absorbance was measured at 540 nm using a microplate reader (VERSA-max™, Molecular Devices, California, USA).

2.5.2. Printability tests

Because the soft denture liner is bonded to the intaglio surface of the denture, we quantified the deviation between the control model (with the designed geometry) and the printed liner attached to the denture base. The overall procedure is illustrated in Fig. 3. Using CAD software, a reference STL file was generated for the maxillary denture base, which was at least 2 mm thick and without teeth. A 5 mm-diameter reference sphere was positioned in the anterior region, and two additional spheres were placed bilaterally in the posterior region to form a triangle for subsequent alignment. Twelve bases were printed using a 3D-printable resin (THD P-1000, Graphy Inc., Seoul, Korea) using a DLP 3D printer. Each specimen was then coated with a scan spray (Easy Scan, Alphadent, Goyang, Korea) and scanned using a laboratory scanner (Freedom HD, DOF Inc., Seoul, Korea) to obtain reference scan data. Next, approximately 1 mm of the intaglio surface was removed using a round denture bur, and the specimens were re-scanned. The Boolean difference function in the CAD software (Blender 4.4.0, Blender foundation, Amsterdam, Netherlands) was used to extract the STL file corresponding to the removed volume. The STL file was printed, washed with alcohol, attached to the intaglio surface of each specimen, and post-polymerized. Varnish (Graphy TC-85, Graphy Inc., Seoul, Korea) was applied to the surface to reduce surface tackiness and porosity. The relined specimens were scanned again using a scan spray and laboratory scanner to obtain the test scan data. To calculate the deviation from the original model and related denture, two sets of scan data were imported into Geomagic Control X software (3D Systems, North Carolina, USA). Initial and best-fit alignments were performed using the three reference spheres, followed by 3D comparative analysis to calculate the root mean square (RMS) difference between the two datasets and quantify the deviation. After measuring the RMS and number of comparison points for each specimen, the weighted RMS and mean RMS were calculated.

3. Results

3.1. Synthesis of urethane-acrylate oligomers

After the reaction of the polyol with isocyanate to produce an isocyanate-terminated urethane, the –NH stretching band was observed at 1530 cm^{-1} (Fig. 4). Completion of the capping reaction was confirmed by the disappearance of the –NCO stretching band at 2270 cm^{-1} and the appearance of an –OH stretching band at 3500 cm^{-1}.

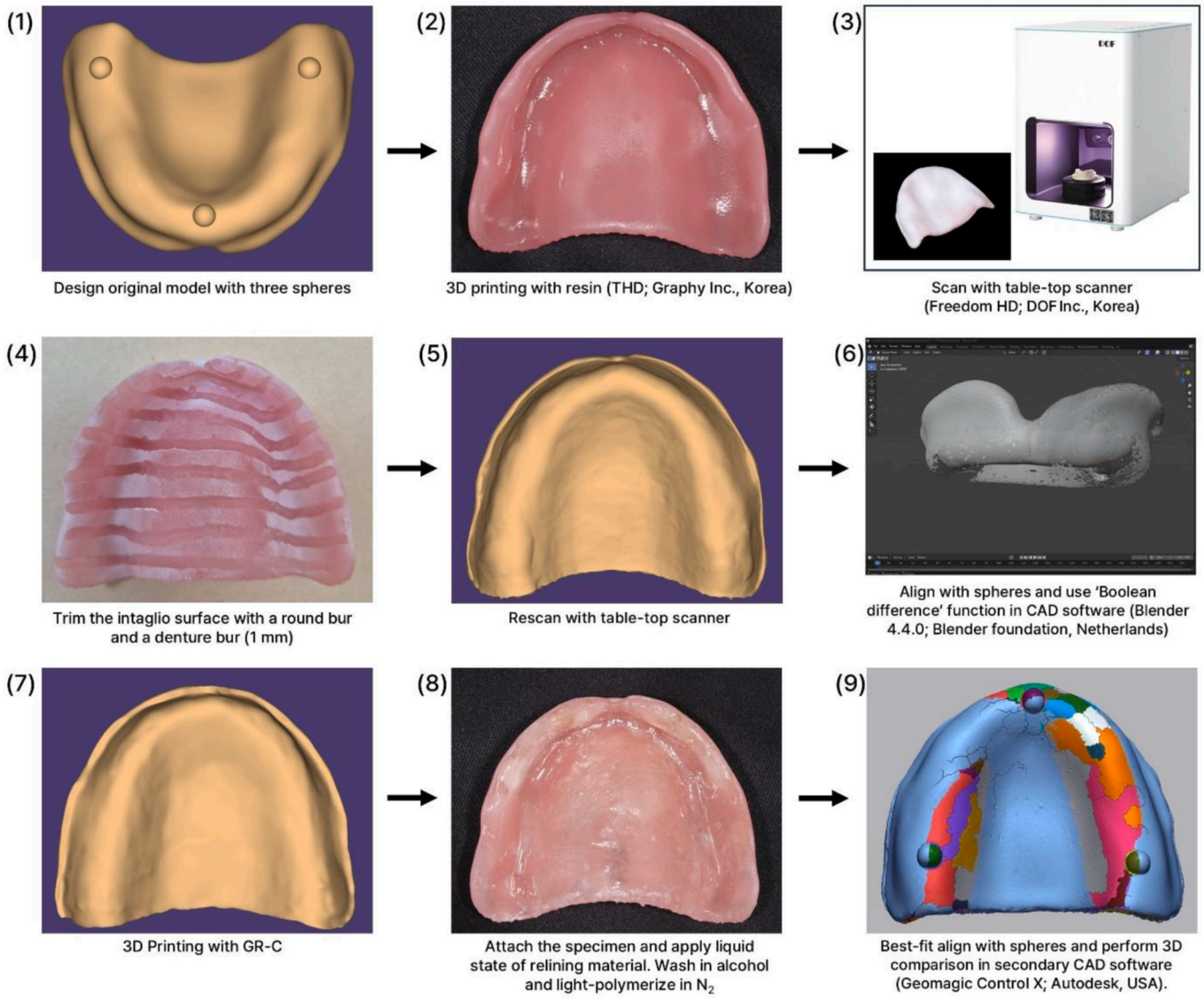

Fig. 3. Workflow for fabricating a 3D-printed relining material for the maxilla. A tabletop scanner (Freedom HD; DOF Inc., Korea) and CAD software (Blender 4.4.0; Blender Foundation, Netherlands) were used for digital acquisition and design. The manually trimmed inner area was subsequently converted into a GR-C denture liner.

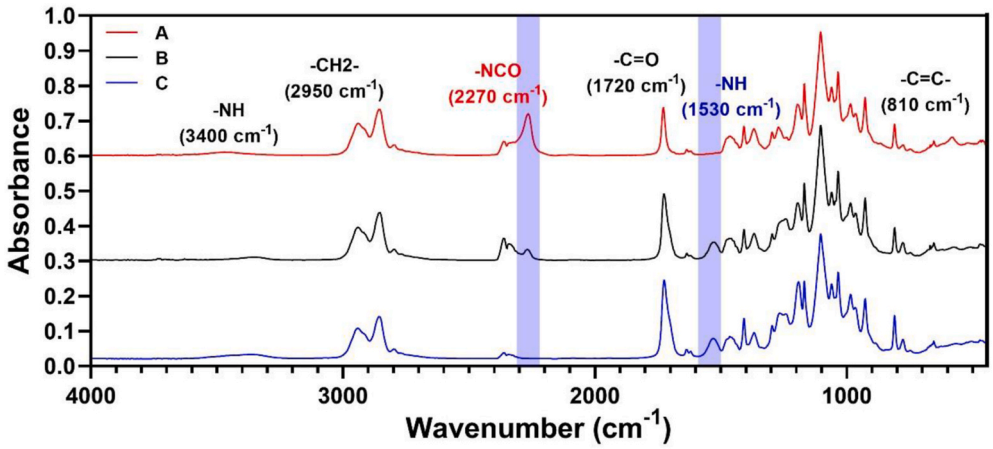

Fig. 4. FT-IR spectra of 1K oligomer (GR-A) recorded during the synthesis process in sequential stages. (A) diol and isocyanate before the urethane reaction. (B) NCO-terminated urethane after the urethane reaction. (C) urethane acrylate oligomer after capping completed.

The synthesis processes for both oligomers (1K: 12900 g/mol, 2K: 18500 g/mol) were verified using the same method. These features demonstrate the successful synthesis of the urethane-acrylate oligomers.

3.2. Comparative evaluation of five different mixing ratios

3.2.1. Tensile properties

Table 2 and Fig. 5 present the results of the tensile tests. The average tensile strengths of the CS (0.312 ± 0.053 MPa) and CC (0.145 ± 0.017 MPa) groups are significantly lower than those for the other groups ($P < 0.01$). Although Fig. 5(b)) implies an increase in tensile strength with increasing 2K oligomer content, i.e., GR-A (0.869 ± 0.22 MPa), GR-B (1.080 ± 0.20 MPa), GR-C (1.128 ± 0.29 MPa), GR-D (1.102 ± 0.063 MPa), and GR-E (1.222 ± 0.14 MPa), these differences are not statistically significant, and the strengths are similar to that of RL2 (1.164 ± 0.26 MPa), as shown in Fig. 5(a).

Statistically significant differences are observed in elongation (Fig. 5 (c) and (d)). In subset a (Table 2), CS (188.65 ± 28.685%) and RL2 (183.97 ± 23.385%) exhibit significantly higher rates of elongation than GR-A (104.21 ± 26.258%), which is the only group in subset c. GR-B (137.92 ± 11.520%), GR-C (143.25 ± 15.890%), and GR-D (151.90 ± 4.3759%) are classified into subsets bc and abc, respectively, indicating intermediate-performing groups. GR-E (164.15 ± 6.2053%) and CC (160.90 ± 13.795%) are included in subset ab, showing no significant difference from the highest-performing groups (CS and RL2) but also overlapping with the intermediate subset. As shown in Fig. 5(d), the elongation tends to increase as the 2K oligomer content increases.

The stress-strain curves of the groups (Fig. 5(e)) indicate that the RL2 and the GR series exhibit elastomeric characteristics, whereas the CS and CC groups demonstrate predominantly plastic deformation. Only the CC groups exhibit deformation beyond their ultimate tensile strengths.

3.2.2. Dynamic mechanical properties

Amplitude sweeps were performed to confirm the validity of the measurements at strains greater than 0.1%, because the plateau tendency indicated that the linear viscoelastic range was maintained (Fig. 6 (a) and (b)). Fig. 6(c), (d), and (e) show the variations in E', E'', and tanδ with temperature, respectively. Most groups show similar overall trends, with a steady decrease in E' and E'' at approximately −60 °C, whereas RL2 exhibits a sharp drop in E' and E'' at −45 °C. In the GR series, from −30 °C to 15 °C, both E' and E'' increase with increasing 2K oligomer content (from GR-A to GR-E). However, at 23.5–32.5 °C, GR-C and GR-B exhibit higher E' values, and at higher temperatures, the trend reverses and the E' values decrease from GR-A to GR-E (Fig. 6 (c)). Above 24.5 °C, GR-C exhibits the highest E'' values (Fig. 6(d)).

The main tanδ peaks are observed near 0 °C (−1.6 to −0.4 °C) for all GR series, and the peak amplitude decreases with increasing 2K oligomer content. The commercial acrylic liner materials (CC and CS) show similar low-temperature peaks (−7.4 to −0.6 °C), whereas the silicone liner material (RL2) exhibits a substantially lower peak temperature (−39.6 °C). The GR-E group exhibits a secondary tanδ peak at 25.5 °C.

Table 3 shows the E', E'', and tanδ values for the different groups at 36.5 °C. The E' values of the GR series decrease with increasing 2K oligomer content. Compared with the commercial silicone liner (RL2), the GR series exhibits higher tanδ values, implying superior damping properties. The bulk modulus (K) was calculated from E', based on the assumption of near-incompressibility of the soft materials, with a Poisson's ratio (ν) of approximately 0.49 for the GR series and RL2, and 0.33 for CC and CS (Eq. (6)).

$$E' = 3K(1-2\nu) \tag{6}$$

3.2.3. Durometer Shore A hardness

Table 4 presents the results of the GLMM analysis. The fixed-effects test results reveal highly significant differences between the groups ($P < 0.001$). In contrast, the main effects of time ($P = 0.631$) and the interaction between group and time ($P = 0.216$) are not significant. According to the fixed coefficients, GR-E and GR-D exhibit significantly lower Shore A hardness values than GR-A ($P < 0.001$). The GR-B and GR-C groups show no statistically significant differences compared to the reference group. The main effects of time and most of the interaction terms are not significant.

After 1 day, GR-A, GR-B, and GR-C are classified as soft, whereas GR-D and GR-E are classified as extra-soft. After 30 days, all five groups are classified as extra-soft (Fig. 7). The Shore A hardness of GR-E is the lowest among the five mixing ratios, but is not significantly different from that of GR-D at 1 or 30 days (Table 5).

3.2.4. Optical rheometry results

Fig. 8 shows the optical rheometry test results. A plateau region is observed after 100 s for all groups. GR-A exhibits the highest E', while GR-E exhibits the highest E''. Increasing the 2K oligomer content results in a decrease in E', whereas both E'' and tanδ increase. The peak in tanδ is delayed as the 2K oligomer content increases.

Table 2
Kruskal-Wallis analysis and post-hoc test result of tensile strength and elongation (a, b, c: $P < 0.05$).

	Group	N	Mean	Standard Deviation	95% Confidence Interval		Minimum	Maximum
					Lower	Upper		
Tensile Strength (MPa)	CS	7	0.31219[b]	0.053242	0.26295	0.36143	0.2221	0.38519
	CC	7	0.14517[b]	0.016761	0.12967	0.16067	0.12644	0.16711
	RL2	7	1.1639[a]	0.26415	0.91964	1.4082	0.7819	1.5524
	GR-A	7	0.86880[a]	0.22310	0.66247	1.0751	0.69054	1.2595
	GR-B	7	1.0798[a]	0.19580	0.89875	1.2609	0.77459	1.3648
	GR-C	7	1.1277[a]	0.29157	0.85807	1.3974	0.75586	1.4151
	GR-D	7	1.1022[a]	0.063071	1.0439	1.1606	1.0472	1.2114
	GR-E	7	1.2219[a]	0.13516	1.0969	1.3469	0.93024	1.3418
	Total	56	0.87772	0.42819	0.76305	0.99239	0.12644	1.5524
Elongation (%)	CS	7	188.65[a]	28.685	162.13	215.18	156.34	233.22
	CC	7	160.90[ab]	13.795	148.14	173.66	142.95	178.79
	RL2	7	183.97[a]	23.385	162.34	205.6	140.56	210.61
	GR-A	7	104.21[c]	26.258	79.926	128.4943	85.67	148.11
	GR-B	7	137.92[bc]	11.520	127.27	148.5752	115.61	151.49
	GR-C	7	143.25[abc]	15.890	128.55	157.9443	120.97	157.43
	GR-D	7	151.90[abc]	4.3759	147.85	155.9486	148.37	160.97
	GR-E	7	164.15[ab]	6.2053	158.41	169.8892	152.53	172.85
	Total	56	154.37	30.718	146.14	162.5960	85.67	233.22

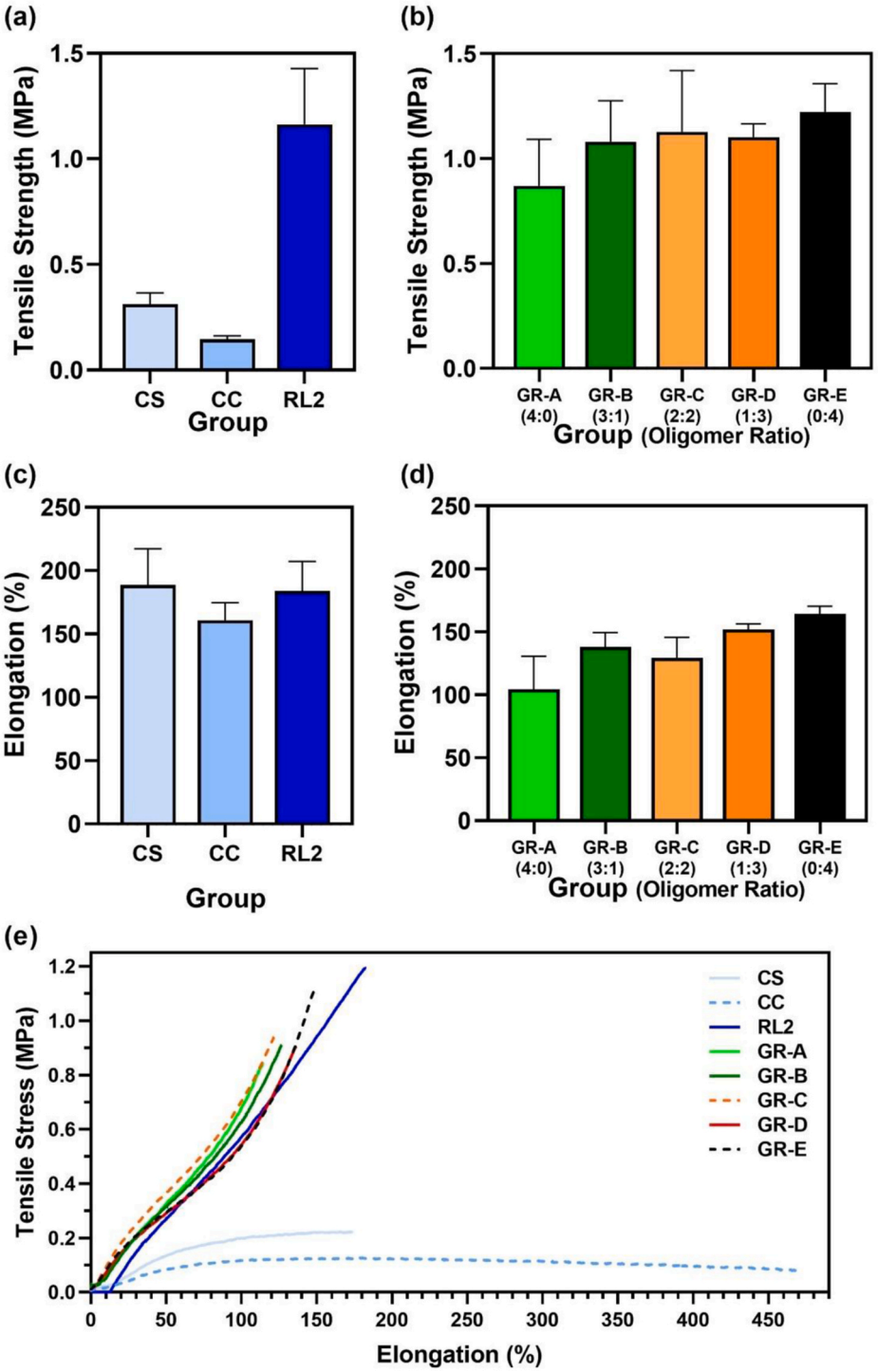

Fig. 5. Tensile test results for each group. Tensile strength (MPa) of (a) commercial denture liner material (CS, CC, and RL2) and (b) synthesized denture liner materials (GR-A, GR-B, GR-C, GR-D, and GR-E). Elongation (%) of (c) commercial denture liners and (d) synthesized liner materials. (e) Stress-strain curve of all tested denture lining materials.

3.2.5. *Dimensional accuracy*

Visual inspection indicated that GR-E exhibits the highest opacity among the groups (Fig. 9(a)–(e)). GEE analysis revealed a significant main effect of deviation for both groups ($P < 0.001$) and axes ($P < 0.001$), as well as for their interaction ($P = 0.002$) (Table 6). Groups GR-A and GR-D exhibit greater deviations than the other GR series. In addition, the x- and y-axes exhibit higher deviations relative to the z-axis (Fig. 9(f)–(h)). Some interactions are observed, with a significantly lower deviation for the GR-C group on the x-axis ($P = 0.032$) and for GR-D on both the x- and y-axes ($P < 0.001$).

3.2.6. *Compressive test results*

The compressive test results are summarized in Table 7. No specimen exhibited fracture within the tested strain range; therefore, compressive stress values at predefined strain levels of 10%, 25%, and 30% were recorded. For all material groups, compressive stress increased with increasing strain. In addition, materials with a higher 1K ratio showed higher compressive stress values across all strain levels. Because

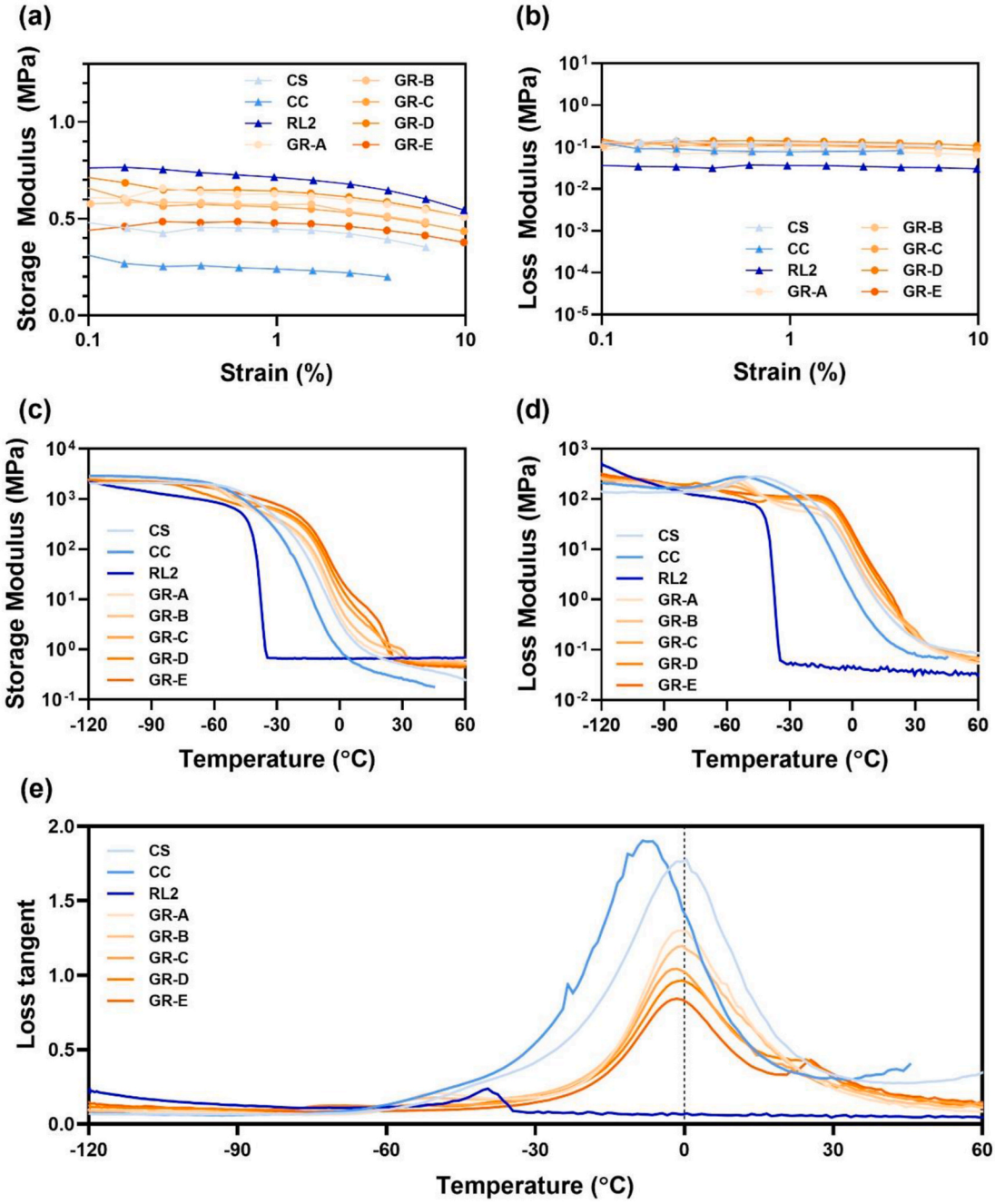

Fig. 6. Dynamic mechanical analysis (DMA) results with (a-b) strain sweep and (c-e) temperature sweep for each group. (a,c) storage modulus. (b,d) loss modulus. (e) loss tangent.

Table 3
Rheological parameters measured near 36.5 °C during dynamic mechanical analysis with temperature variation.

Group	Temperature (°C)	E' (MPa)	E'' (MPa)	E^* (MPa)	tanδ	K (MPa)	Poisson's Ratio (ν)
CS	36.66	0.436	0.125	0.4536	0.2866	0.3790	0.33
CC	36.52	0.2318	0.0753	0.2437	0.3246	0.2015	0.33
RL2	36.56	0.669	0.034	0.6699	0.0508	11.08	0.49
GR-A	36.53	0.6466	0.109	0.6557	0.1685	10.70	0.49
GR-B	36.56	0.617	0.1225	0.6290	0.1985	10.21	0.49
GR-C	36.62	0.5624	0.1247	0.5761	0.2217	9.311	0.49
GR-D	36.52	0.5495	0.1225	0.5630	0.223	9.097	0.49
GR-E	36.55	0.5049	0.1234	0.5198	0.2444	8.359	0.49

compressive stress values deviated from normality, the data were log-transformed prior to LMM analysis. At each strain level, GR-A, GR-B and GR-C showed significantly higher compressive stress than groups GR-D, GR-E ($P < 0.05$, Holm-adjusted).

Table 4
Shore A harness test statistics.

Source	F	df1	df2	Significance (*P*-value)
Corrected model	25.031	9	50	<0.001
Group	39.277	4	50	<0.001
Day	0.234	1	50	0.631
Group*Day	1.501	4	50	0.216

Model term	Regression Coefficient	Standard Error	t-value	Significance (*P*-value)	95% Confidence Interval	
					Lower	Upper
Intercept	28.741	0.8001	35.920	<0.001	27.134	30.348
GR-E	−12.082	1.1316	−10.677	<0.001	−14.354	−9.809
GR-D	−6.299	1.1316	−5.567	<0.001	−8.572	−4.027
GR-C	−1.944	1.1316	−1.718	0.092	−4.217	0.329
GR-B	−0.834	1.1316	−0.737	0.465	−3.107	1.439
GR-A	0[b]	.	.	.	.	.
Day	−0.042	0.0627	−0.665	0.509	−0.168	0.084
day*[GR-E]	0.191	0.0886	2.150	0.036	0.013	0.369
day*[GR-D]	0.035	0.0886	0.394	0.695	−0.143	0.213
day*[GR-C]	0.023	0.0886	0.262	0.794	−0.155	0.201
day*[GR-B]	0.028	0.0886	0.311	0.757	−0.150	0.206
day*[GR-A]	0[b]	.	.	.	.	.

Distribution: Normal.
Link function: Identity.
a. Dependent variable: hardness.
b. This parameter is redundant and set to zero.

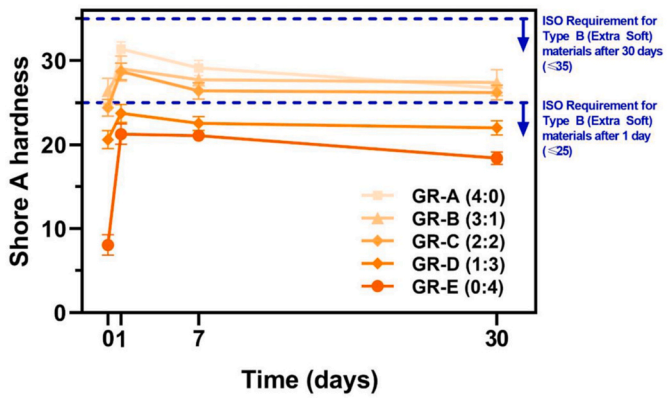

Fig. 7. Shore A hardness of five different polyurethane-urethane acrylate soft denture liner materials (GR-A, GR-B, GR-C, GR-D, and GR-E) measured after 0 day, 1 day, 7 days, and 30 days.

Table 5
Shore A hardness at 37 ± 1 °C measured after 1 day and after 30 days.

Group	after 1 day		after 30 days	
	Mean	S.D	Mean	S.D
GR-A	31.4[a]	0.828	26.7[a]	0.594
GR-B	29.1[a]	0.961	27.4[a]	1.55
GR-C	28.7[a]	1.53	26.2[a]	0.862
GR-D	23.7[b]	0.884	22.0[b]	0.845
GR-E	21.3[b]	0.703	18.4[b]	0.737

Values labeled 'a' and 'b' within the same column differ significantly at the $P < 0.05$ level.

3.2.7. Water sorption and solubility test

GR-D yielded only two specimens and GR-E could not be successfully fabricated in the disc geometry required for ISO 10139-2 testing due to geometry-dependent printability limitations. Therefore, water sorption and solubility analyses were conducted for GR-A, GR-B, and GR-C only.

The results are summarized in Table 8. One-way ANOVA revealed significant differences among groups for both WS ($P < 0.05$) and SL ($P < 0.05$). For WS, GR-A (14.852 ± 0.823 μg/mm^3) and GR-B (14.795 ± 0.491 μg/mm^3) showed significantly higher values than GR-C (13.077 ± 0.447 μg/mm^3), with no significant difference between GR-A and GR-B.

For solubility, GR-A (12.294 ± 1.272 μg/mm^3) exhibited significantly lower values than GR-B (15.047 ± 0.221 μg/mm^3) and GR-C (16.232 ± 0.739 μg/mm^3), while no significant difference was observed between GR-B and GR-C.

3.2.8. Degree of conversion test results

FT-IR analysis showed that the aliphatic C=C peak at 810 cm^{-1} was not detectable after printing and post-polymerization in all groups. Consequently, the calculated degree of conversion values approached 100% at the near surface region for all formulations. These results suggest a high level of surface polymerization under applied conditions. Detailed FT-IR spectra and absorbance ratios are provided in the Supplementary Material (Table S1, Fig. S1).

3.3. Clinical applicability

Considering tensile strength and elongation, GR-C, GR-D, and GR-E exhibited favorable mechanical properties. In terms of rheological behavior, GR-E, composed solely of 2K oligomer, showed the smallest difference in the *K* value compared with that of oral mucosa. However, GR-C, with its higher Shore A hardness and $|E^*|$, resists occlusal forces more effectively. Regarding dimensional accuracy, GR-D demonstrated greater deviation than GR-E and GR-C. Although no specific formulation showed superiority in all aspects, GR-C was selected for further evaluation because, as a denture liner, it must maintain its form and stability over the long term without deformation or displacement from the denture base, ensuring reliable clinical applicability.

3.3.1. Cytotoxicity

Microscopic evaluation revealed no cellular reactivity at any concentration of GR-C (Table 9). In the MTT assay, the cell viabilities at 0, 6.25, 12.5, 25, 50, and 100% extract concentrations are 100, 113, 112, 119, 108, and 97%, respectively, which are well below the 30% cytotoxicity threshold specified in the ISO 10993-5:2009 quantitative evaluation guidelines. Accordingly, based on both qualitative and quantitative assessments, GR-C was deemed non-cytotoxic under the conditions used in this study.

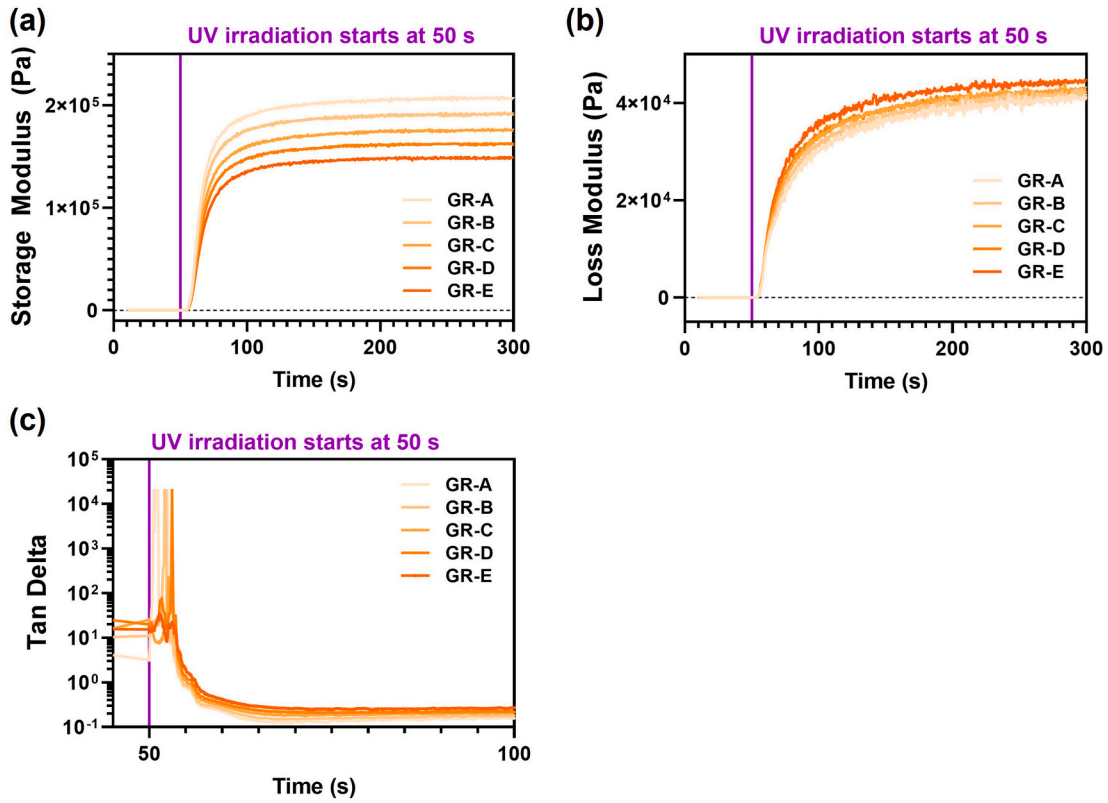

Fig. 8. UV rheology results showing time-dependent response of five denture liner materials, with UV irradiation starting at 50 s. (a) storage modulus (Pa), (b) loss modulus (Pa), and (c) loss tangent with respect to time (s).

3.3.2. *Printability*

The printed soft denture liner after attachment to the intaglio surface of the denture is shown in Fig. 10. The minimum and maximum deviations are 0.449 and 0.735 mm, respectively. The weighted RMS of the surface deviation is 0.619 mm, calculated from 402835 sampled points across the 12 specimens. The central tendency is 0.613 ± 0.082 (mean ± standard deviation; 95% confidence interval = 0.561–0.666). Specimens 5 and 12 represent the lower and upper bounds, which lie within the expected variation, so exclusion is not warranted. Fig. 9(i) shows a color map of the 3D comparison. The green area represents the tolerance range (0.20 mm), indicating that the liner was fabricated similarly to the original denture. The blue areas show where the liner is thinner, while the red areas indicate regions where it is thicker compared to the original denture. The greatest deviations were observed in the anterior alveolar ridge and posterior flange regions, whereas the palatal area exhibited the closest resemblance.

4. Discussion

4.1. *Clinical rationale & biomechanical compatibility*

Patients who use complete dentures or removable partial dentures for extended periods frequently complain of decreased soft tissue retention and traumatic lesions (Bilhan et al., 2012, 2013; Shiga et al., 2007; Tallgren, 2003). To address this, dentists regularly reline their dentures. Since existing soft denture liners have disadvantages that limit their semi-permanent use, clinicians must switch to hard denture liners. However, patients with maxillofacial defects or those who have worn dentures for a long time may have insufficient alveolar support for dentures, and those with undercuts have reported difficulty and discomfort when wearing dentures with rigid tissue surfaces (Mitra et al., 2014). New materials that can be used longer than conventional soft denture liners are required for these patients.

An ideal soft denture liner should maintain its physical properties during long-term clinical use and be stable in the oral environment. The material must possess sufficient strength while maintaining the appropriate viscoelasticity and biocompatibility. Although no definitive clinical guidelines currently exist regarding the viscoelastic requirements of intraoral relining materials, previous studies have suggested that soft denture liners should possess elastic moduli comparable to those of the oral mucosa, as they are intended to replace lost tissue (Abe et al., 2009). At the same time, a higher E' may enhance the ability of soft-lined dentures to crush food instantaneously (Murata et al., 2008). Therefore, the elastic modulus of the liner should be comparable to that of the oral mucosa while remaining sufficiently high to maintain functional stability. Additionally, to reduce the occlusal load transmitted to the underlying tissues, the liner should exhibit a higher damping factor (tanδ), enabling greater dissipation of mechanical energy during mastication. However, increased viscosity may affect the extent of irreversible deformation. As a result, it should not favor either aspect and must demonstrate superior performance in both to ensure compatibility with the oral mucosa.

The physical properties and viscoelasticity, which depend on the composition of the two oligomers, were compared to evaluate the suitability of these materials as soft denture liners. As the 2K oligomer content increases, the elongation at the ultimate tensile strength tends to increase. Although the ultimate tensile strength is not statistically different between groups, the maximum and minimum values steadily increase (Fig. 5(b)), and the standard deviation tends to decrease (Table 2). These results indicate that a higher 2K oligomer content enhances the mechanical strength of the material during tensile loading.

In all GR series, Shore A hardness stayed within the range specified by the ISO for maintaining softness, and GR-D and GR-E, with the highest content of 2K oligomers, are categorized as extra-soft (Fig. 7). This indicates that all groups satisfy the softness level required by soft denture liners. However, GR-E and GR-D exhibit significantly lower

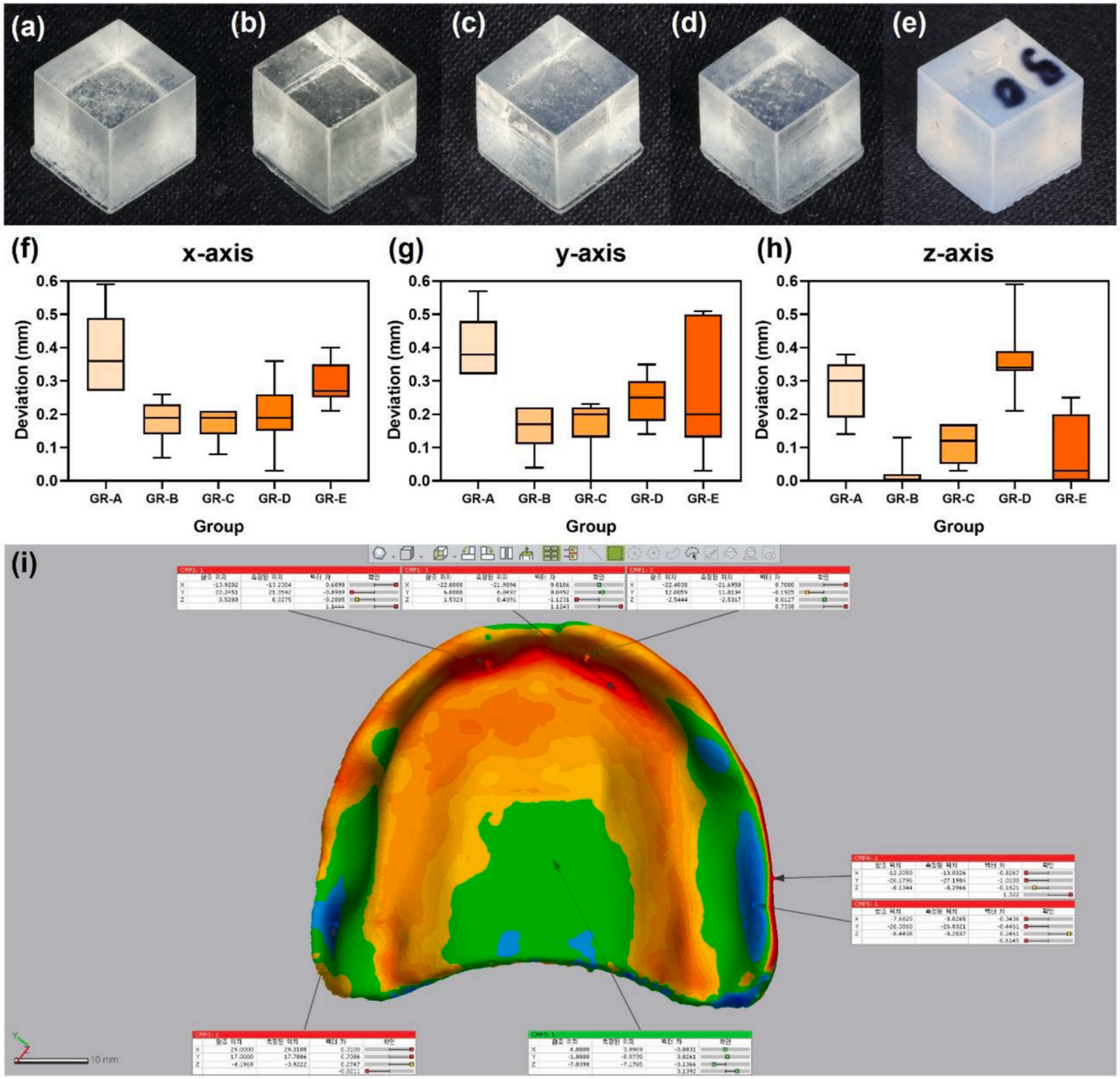

Fig. 9. (a-e) Printed cubic specimens: (a) GR-A, (b) GR-B, (c) GR-C, (d) GR-D, (e) GR-E. (f-h) Box plots for deviations from (a) x-axis (b) y-axis, and (c) z-axis for each group. (i) Color map of 3D comparison analysis after superimposition of original model and scanned data of 3D printed denture. The blue areas show where the liner is thinner, while the red areas indicate regions where it is thicker compared to the original denture. (For interpretation of the references to color in this figure legend, the reader is referred to the Web version of this article.)

hardness values than GR-A, whereas GR-B and GR-C show no significant differences from GR-A.

The DMA and optical rheometry results show that the 2K oligomer has a higher viscosity than the 1K oligomer, which increases tanδ but decreases $|E^*|$ (Figs. 5 and 7). The E' of the oral mucosa ranges from 0.37 to 5.93 MPa (Inoue et al., 1985; Isobe et al., 2013; Tanaka, 1973). In all experimental groups in this study, except for CC, the E' values measured at 36.5 °C are within this range (Table 3). In previous research, K was calculated using the E' and ν values for a soft denture liner, and its similarity to the compression modulus of the oral mucosa was evaluated (Lacoste-Ferré et al., 2011). Similar to the referenced study, we calculated K for commercial soft denture liners and GR series by assuming ν values of 0.33 for amorphous polymers and 0.49 for elastomers (Van Krevelen and te Nijenhuis, 2009), which showed that the K of the GR series exceeds that of the oral compression modulus. As the 2K oligomer content increases, K decreases.

Under compressive loading, polyurethane tends to exhibit viscoelastic deformation, such as creep or viscous flow, rather than catastrophic failure, particularly at lower height-to-length ratios (Li et al., 2020). Consistent with this behavior, no specimen fracture was observed in the present study. Because excessive deformation of elastomeric liners may lead to vertical displacement of the denture and patient discomfort, compressive stress at 10%, 25%, and 30% strain was evaluated to provide clinically relevant reference data. As the 1K oligomer content increased, the compressive load required to induce deformation increased. Although functional occlusal forces may result in measurable

Table 6
Dimensional accuracy test statistics.

Source	Wald Chi-square	df	Significance (*P*-value)
Corrected model	751.842	1	<0.001
Group	125.440	4	<0.001
axis	12.396	2	0.002
Group*axis	30.698	8	<0.001

Parameter	Regression Coefficient	Wald Chi-square	df	Significance (*P*-value)	95% Wald Confidence Interval	
					Lower	Upper
Intercept	0.111	13.088	1	<0.001	0.051	0.172
GR-A	0.167	15.015	1	<0.001	0.083	0.252
GR-B	−0.047	1.546	1	0.214	−0.121	0.027
GR-C	−1.499E-17	0.000	1	1.000	−0.071	0.071
GR-D	0.250	24.427	1	<0.001	0.151	0.349
GR-E	0[a]	.	.	.	.	.
x-axis	0.184	12.421	1	<0.001	0.082	0.287
y-axis	0.170	7.017	1	0.008	0.044	0.296
z-axis	0[a]	.	.	.	.	.
GR-A*x-axis	−0.069	0.713	1	0.398	−0.228	0.091
GR-A*y-axis	−0.043	0.295	1	0.587	−0.197	0.112
GR-A*z-axis	0[a]	.	.	.	.	.
GR-B*x-axis	−0.066	1.110	1	0.292	−0.188	0.057
GR-B*y-axis	−0.076	1.131	1	0.288	−0.215	0.064
GR-B*z-axis	0[a]	.	.	.	.	.
GR-C*x-axis	−0.129	4.593	1	0.032	−0.246	−0.011
GR-C*y-axis	−0.110	2.162	1	0.141	−0.257	0.037
GR-C*z-axis	0[a]	.	.	.	.	.
GR-D*x-axis	−0.347	21.417	1	<0.001	−0.494	−0.200
GR-D*y-axis	−0.294	13.897	1	<0.001	−0.449	−0.140
GR-D*z-axis	0[a]	.	.	.	.	.
GR-E*x-axis	0[a]	.	.	.	.	.
GR-E*y-axis	0[a]	.	.	.	.	.
GR-E*z-axis	0[a]	.	.	.	.	.
Scale parameter	0.009					

Dependent variable: deformation.
Model: (Intercept), Group, Axis, Group*Axis.
a. This parameter is redundant and set to zero.

Table 7
Compressive stress values at defined strain levels obtained from the compression tests of five specimens in each group.

		GR-A	GR-B	GR-C	GR-D	GR-E
Compressive stress at defined strain (MPa)	10%	0.412[a]	0.398[a]	0.390[a]	0.356[b]	0.353[b]
	25%	1.107[a]	1.039[a]	1.066[a]	0.959[b]	0.977[b]
	30%	1.597[a]	1.506[a]	1.575[a]	1.462[b]	1.450[b]

Values labeled 'a' and 'b' within the same row differ significantly at the $P < 0.05$ level.

Table 8
Water sorption (WS) and solubility (SL) of GR-A, GR-B, and GR-C. Values are presented as mean ± standard deviation (n = 5).

	GR-A	GR-B	GR-C
Water sorption (WS, μg/mm^3)	14.852 ± 0.823[a]	14.795 ± 0.491[a]	13.077 ± 0.447[b]
Solubility (SL, μg/mm^3)	12.294 ± 1.272[a]	15.047 ± 0.221[b]	16.232 ± 0.739[b]

Values labeled 'a' and 'b' within the same row differ significantly at the $P < 0.05$ level.

deformation of a 1 mm thick liner, further investigation is needed to determine the clinical significance of such deformation, considering mucosal compliance and load distribution through the denture base.

4.2. Material design & molecular mechanism

The characteristics of polyurethane-acrylates are influenced by the type of polyol, diisocyanate, capping agents, curing conditions, and reactive diluents used in their preparation (Maurya et al., 2018).

Increasing the proportion of 2K oligomers expands the soft segment region, enhancing chain mobility and ductility (Dębowski and Balas, 2000; Lee et al., 1999; Yoo et al., 2001). At the same time, intermolecular hydrogen bonding within urethane segments may introduce reversible physical crosslinking interactions, limiting excessive chain flow (Chen et al., 1996; Nakazato et al., 1989; Szycher, 2012; Yoo et al., 2001; Zhou et al., 2018). This molecular duality, that is, greater segmental flexibility and transient network strengthening, may account for the observed increase in elongation and the simultaneous increase in tensile strength retention from GR-A to GR-E.

The secondary tanδ peak observed around 25 °C for GR-E may reflect restricted segmental motion within partially ordered or phase-separated domains which may enhance dimensional stability and energy dissipation under masticatory loads (Gisselfält and Helgee, 2003). The higher opacity of GR-E may be associated with enhanced microphase separation or increased heterogeneity within the polymer network. Confirmation would require complementary thermal and structural analyses, such as differential scanning calorimetry and X-ray diffraction.

The photoinitiator in this study is a Type I photoinitiator, which generates radicals more efficiently than Type II photoinitiators, resulting in faster polymerization and potentially higher mechanical strength (Almeida et al., 2020; Kowalska et al., 2021). Omnirad 819 has a broad absorption range between 365 and 416 nm, and we used a 405 nm light source for polymerization (Meereis et al., 2014; Niedźwiedź et al., 2023). FT-IR with ATR mode indicated a high near-surface degree of conversion after post-processing, suggesting that surface double-bond consumption was largely completed. Nevertheless, Shore A hardness of all GR series (especially GR-E) increased markedly within the first 24 h after post-processing. Because the degree of conversion was already near completion at the surface, this early hardness increase is unlikely to

Table 9
Results of microscopic evaluation and quantitative cytotoxicity assessment of GR-C using the MTT assay (24-h treatment).

Group	Test substance	Concentration (%)	Reactivity (Grade)	Optical Density (540 nm) (Mean ± S.D.)	Viability (%)
Negative control	Cell culture medium	0	None (0)	0.939 ± 0.078	100
Test group	GR-C	6.25	None (0)	1.063 ± 0.138	113
		12.5	None (0)	1.050 ± 0.082	112
		25.0	None (0)	1.115 ± 0.070	119
		50.0	None (0)	1.015 ± 0.065	108
		100	None (0)	0.911 ± 0.152	97.0
Positive control	DMSO	3	Mild (2)	0.422 ± 0.022	45.0[a]
		6	Moderate (3)	0.195 ± 0.027	20.8[a]
		12	Severe (4)	0.114 ± 0.008	12.2[a]

Define Reactivity (Grade).
None (0): Discrete intracytoplasmic granules; no cell lysis.
Slight (1): Not more than 20% of the cells are round, loosely attached, and without intracytoplasmic granules; occasional lysed cells are present.
Mild (2): Not more than 50% of the cells are round and devoid of intracytoplasmic granules; no extensive cell lysis and empty areas between cells.
Moderate (3): Not more than 70% of the cell layers contain rounded cells or are lysed.
Severe (4): Nearly complete destruction of the cell layers.
S.D.: Standard deviation.
Viability (%) = (OD540test/OD540control) x 100.
OD540test is the mean value of measured optical density of the test substance.
OD540control is the mean value of measured optical density of the negative control.
[a] Cytotoxicity ≥30%.

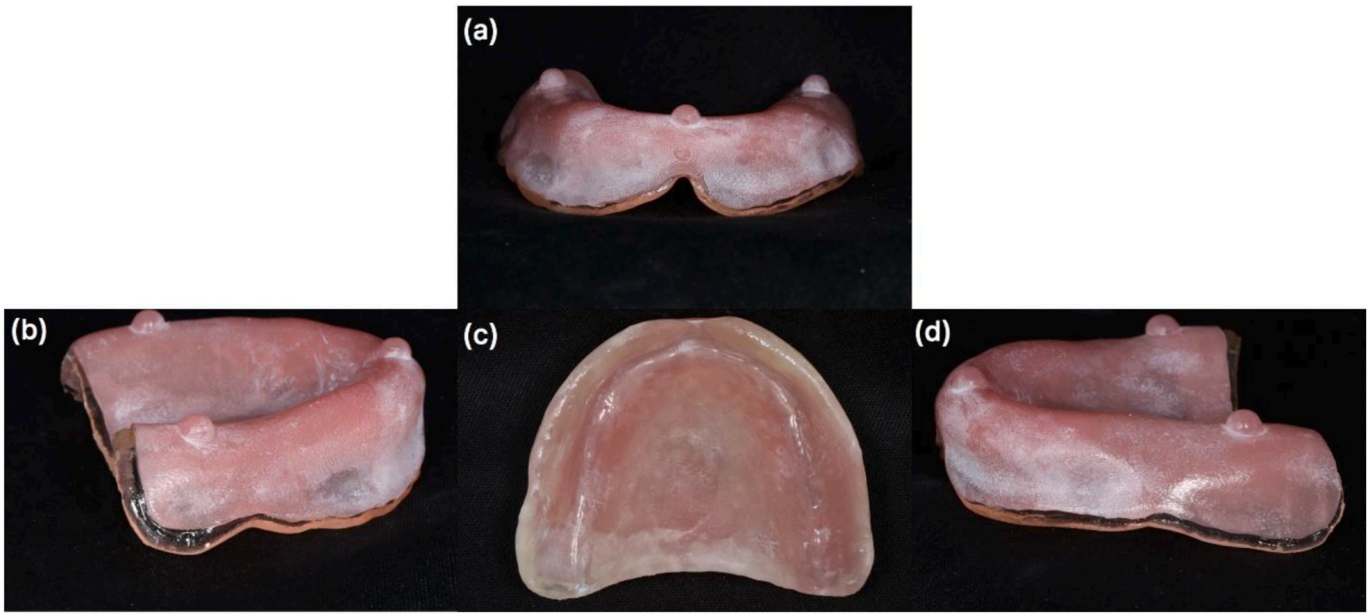

Fig. 10. The completed denture by using denture liner GR-C: (a) frontal view, (b) right oblique view, (c) occlusal view, and (d) left oblique view.

be primarily caused by additional polymerization. Instead, it is more plausibly attributed to delayed network stabilization, including reorganization of urethane hydrogen-bonded domains and microphase structure. In addition, post-immersion extraction of loosely bound low-molecular-weight species may also contribute to reduced chain mobility and increased surface stiffness.

4.3. Printability

From a fabrication standpoint, dimensional accuracy is critical for clinical application. Resin viscosity and network stabilization influence curing kinetics and polymerization-induced shrinkage, thereby affecting print fidelity. GR-B, GR-C, and GR-E exhibited significantly lower overall deformation compared with the other compositions (Table 6). Along the x-axis, GR-C demonstrated less distortion than GR-E (Fig. 9 (f)).

Among the GR formulations, GR-C showed a balanced profile, combining viscoelastic damping within the target range, sufficient resistance to compressive strain compared with softer formulations, and favorable dimensional stability. Based on its balanced mechanical and viscoelastic profile, GR-C was selected for printability assessment.

Because there have been no prior reports to develop soft denture liners through 3D printing, this study demonstrated the fabrication of soft denture liners by printing GR-C (Fig. 3). A deviation of approximately 0.619 mm was observed on the tissue surface compared to the state before liner application. The actual change in the oral mucosa is approximately 0.3 mm (Ishinabe, 1991; Lytle, 1962); therefore, the measured deviation is greater than this value. However, because the characteristics of soft lining materials can lead to displacement due to external forces, and the oral mucosa can be easily deformed under compression, this margin of error may not necessarily cause problems during denture use. Previous reports have indicated that deviations of up

to 1 mm may occur when relining the denture with soft denture liners (Kamal, 2025). Further research is needed to determine whether this deviation is problematic in a clinical situation. The color map presented in Fig. 9(i) shows that the deviations occur mainly at the edges and in the narrow curves of the anterior part, which appears to be due to sagging caused by the layer-by-layer stacking method of DLP printing (Alqutaibi et al., 2025; Šimunović et al., 2025; Zhu et al., 2022). As DLP-based 3D printing has been shown to produce highly complex structures with high resolution and compatibility with a wide range of soft materials, additional studies are necessary to identify the optimal printing conditions that can minimize these errors (Ge et al., 2022).

4.4. Stability & biological safety

Water sorption and solubility were evaluated with reference to ISO 10139-2:2016. However, the specimen thickness was modified to accommodate the minimum dimensions required for stable 3D printing. GR-A exhibited the highest water sorption and lowest solubility, whereas GR-C showed the opposite trend. The increased proportion of the long-chain 2K oligomer may have influenced network architecture, potentially limiting bulk water diffusion while permitting the presence of extractable low-molecular-weight fractions.

After unit conversion, previously reported 1-week water sorption values ranged from 4.6 to 111.4 μg/mm^3 (Kawano et al., 1994a,b), and the present GR formulations (13–15 μg/mm^3) fall within this range. Although the solubility values (12–16 μg/mm^3) are higher than those reported for some conventional soft lining materials (0.6–8.0 μg/mm^3), the degree of conversion was near complete, consistent with minimal unreacted monomer content. The elevated solubility may therefore be attributed to the release of low-molecular-weight fractions inherent to the flexible polyurethane network rather than ongoing hydrolytic degradation.

When solubility is high, attention must be paid to cytotoxicity. The cytotoxicity of polyurethane acrylates based on urethane–acrylate oligomers varies depending on the type of monomer and oligomer used. Previous studies on the biocompatibility of urethane-acrylate oligomers evaluated composites containing urethane dimethacrylate using MTT assays (Bean et al., 1995; Goël Brackett et al., 2007; Sigusch et al., 2007). A previous study using photoinitiators and urethane-acrylate oligomers, similar to the present study, also assessed cytotoxicity using MTT assays (Kanie et al., 2009). Therefore, the cytotoxicity of GR-C was quantitatively evaluated using the MTT assay and qualitatively evaluated using microscopy. Since no cytotoxicity was observed, the preliminary suitability of GR-C as a soft denture liner was demonstrated.

Shore A hardness did not exhibit statistically significant deterioration after the initial conditioning period. Previous studies have also shown that water-induced mechanical changes in elastomeric polyurethane systems largely stabilize within 24 h of immersion (Schwarz et al., 2022). Taken together, these findings suggest that the observed solubility did not result in measurable short-term mechanical or biological instability under the tested conditions, although extended aging studies would further clarify long-term stability.

4.5. Comparison with commercial materials and clinical implications

Compared with the GR group, the commercial soft denture liners CC and CS exhibit distinct tendencies, whereas RL2 demonstrates similar tendencies. The elongation at break of CC is the highest among all groups (Fig. 5(e)). CC is an acrylic-based soft denture liner used as a tissue conditioner; therefore, it must be easily deformed by occlusal forces for good adaptation. Owing to this low consistency, at 36.5 °C, CC shows the highest tanδ and the lowest $|E^*|$ and E' values (Table 3), which are similar to those presented in a previous study (Lacoste-Ferré et al., 2011). RL2 is a silicone-based elastomer, which exhibits high elongation and tensile strength, as indicated by its stress–strain curve (Fig. 5(e)). Therefore, RL2 shows the highest $|E^*|$ and smallest tanδ (Table 3), implying a strong resistance to external occlusal forces but a limited ability to reduce the force transmitted to the underlying oral tissues. Although the GR series exhibits elastomeric characteristics similar to those of RL2 (Fig. 5(e)), it shows more than a threefold higher E' and tanδ at 36.5 °C, indicating superior damping ability compared with RL2.

Accordingly, the previously selected GR-C formulation, unlike conventional acrylic-based long-term soft denture liners, maintained stable Shore A hardness over time while exhibiting higher tensile strength. In contrast to silicone-based materials, GR-C combined the mechanical stability of an elastomer with enhanced viscous behavior, thereby facilitating effective attenuation of occlusal forces. Importantly, its moldless fabrication through digital printing enables application to complex geometries that are difficult to achieve with conventional processing methods.

4.6. Summary & further research & limitation

This study aimed to overcome the drawbacks of conventional soft denture liners by utilizing polyurethane and incorporating 3D printing using a photoinitiator to facilitate processing. To this end, the entire process was demonstrated, from the synthesis of the urethane-acrylate oligomer to the 3D printing of a soft denture liner. During this process, it was confirmed that the mechanical properties and viscoelastic properties obtained by varying the ratio of the synthesized oligomers are similar to or better than those of existing materials. Most importantly, conventional materials need to be manually mixed by clinicians, leading to differences in the final product depending on the skill level of the clinician. Even if the physical properties of the initial materials are excellent, the inherent limitations of the material inevitably result in plasticizer leaching and adhesive failure. Ultimately, this leads to increased cost and time burdens for both clinicians and patients. The soft denture liner proposed in this study cannot be fabricated directly in the oral cavity; however, it eliminates the need for separate mixing of materials and exhibits excellent material homogeneity and stability of the final product.

The main limitation of this study is that the evaluation of the developed soft denture liner was performed solely at an in-vitro level. The intraoral environment is characterized by persistent moisture, temperatures maintained at approximately 37 °C or higher than ambient conditions, the presence of diverse oral microorganisms, mobility of the underlying mucosa, and exposure to masticatory forces. Therefore, it is necessary to verify whether the physical properties of the soft denture liner can be stably maintained over a prolonged period under conditions that closely simulate the oral environment.

In addition, although printability was assessed in this study using a 3D-printed denture base, heat-polymerized PMMA denture bases are still more commonly used in clinical practice. Accordingly, further studies are required to evaluate the bonding strength between different types of denture base materials and the soft denture liner fabricated using the urethane acrylate oligomer developed in this study. Moreover, because the mechanical properties and printing accuracy of 3D-printed materials may be affected by post-processing conditions, additional investigations are needed to determine optimal post-processing protocols (Piedra-Cascón et al., 2021). Finally, to facilitate clinical application, standardized protocols for support removal after 3D printing, varnish application, and trimming of excess or elongated areas should be established.

5. Conclusion

This study presents the first report of a polyurethane–acrylate soft denture liner that can be directly fabricated using 3D printing. Two types of urethane acrylate oligomers were synthesized, and their compositions were systematically evaluated in terms of mechanical, rheological, and dimensional properties compared with conventional soft

denture liners. Through this process, a compositionally optimized formulation (GR-C) was developed. The optimized formulation exhibited no cytotoxicity in the MTT assay. Although additional research is required to optimize printing conditions for improved dimensional accuracy, these results demonstrate a novel 3D-printable soft denture liner material and establish a foundation for translating oligomer-level polymer design into functional prosthetic biomaterials. Future studies should focus on assessing long-term adhesion to denture bases, and validating in vivo performance. Overall, this study represents a fundamental step toward the development of next-generation 3D-printable, biocompatible soft denture liner for removable prostheses.

Declaration of generative AI and AI-assisted technologies in the manuscript preparation process

During the preparation of this manuscript, the authors used ChatGPT for language editing and grammar refinement. After using this tool, the authors carefully reviewed and revised the content as necessary and take full responsibility for the final published version.

Funding

This research was supported by Basic Science Research Program through the National Research Foundation of Korea (NRF) funded by the Ministry of Education(No.RS-2023-00242473).

CRediT authorship contribution statement

Sangmin Ham: Conceptualization, Data curation, Investigation, Software, Visualization, Writing – original draft. **Jinhong Min:** Data curation, Investigation, Software, Writing – original draft. **Jiho Lee:** Software, Visualization. **Young-Bum Park:** Conceptualization, Methodology, Supervision. **Hoon Kim:** Conceptualization, Data curation, Methodology, Supervision, Writing – review & editing. **Jaehan Park:** Funding acquisition, Methodology, Project administration, Resources, Supervision, Writing – review & editing.

Declaration of competing interest

The authors declare the following financial interests/personal relationships which may be considered as potential competing interests: Jaehan Park reports financial support was provided by Basic Science Research Program through the National Research Foundation of Korea (NRF) funded by the Ministry of Education (No.RS-2023-00242473). If there are other authors, they declare that they have no known competing financial interests or personal relationships that could have appeared to influence the work reported in this paper.

Appendix A. Supplementary data

Supplementary data to this article can be found online at https://doi.org/10.1016/j.jmbbm.2026.107421.

Data availability

Data will be made available on request.

References

Abe, Y., Taji, T., Hiasa, K., Tsuga, K., Akagawa, Y., 2009. Dynamic viscoelastic properties of vinyl polysiloxane denture soft lining materials. J. Oral Rehabil. 36, 887–893. https://doi.org/10.1111/j.1365-2842.2009.02015.x.

Almeida, S.M., Meereis, C.T.W., Leal, F.B., Carvalho, R.V., Boeira, P.O., Chisini, L.A., Cuevas-Suárez, C.E., Lima, G.S., Piva, E., 2020. Evaluation of alternative photoinitiator systems in two-step self-etch adhesive systems. Dent. Mater. 36, 29–37. https://doi.org/10.1016/j.dental.2019.11.008.

Alqutaibi, A.Y., Aljohani, R., Almuzaini, S., Alghauli, M.A., 2025. Physical–mechanical properties and accuracy of additively manufactured resin denture bases: impact of printing orientation. J. Prosthodont Res. JPR_D_24_00263. https://doi.org/10.2186/jpr.JPR_D_24_00263.

Bean, T.A., Zhuangl, W.C., Tongl, P.Y., David Eick, J., Chappelow, C.C., Yourteel, D.M., 1995. Comparison of tetrazolium calorimetric and 51Cr release assays for cytotoxicity determination of dental biomaterials. Dent. Mater. 11, 327–331. https://doi.org/10.1016/0109-5641(95)80029-8.

Bilhan, H., Erdogan, O., Ergin, S., Celik, M., Ates, G., Geckili, O., 2012. Complication rates and patient satisfaction with removable dentures. J. Adv. Prosthodont. 4, 109–115. https://doi.org/10.4047/jap.2012.4.2.109.

Bilhan, H., Geckili, O., Ergin, S., Erdogan, O., Ates, G., 2013. Evaluation of satisfaction and complications in patients with existing complete dentures. J. Oral Sci. 55, 29–37. https://doi.org/10.2334/josnusd.55.29.

Braden, M., Wright, P.S., Parker, S., 1995. Soft lining materials–a review. Eur. J. Prosthodont. Restor. Dent. 3, 163–174.

Charlon, M., Heinrich, B., Matter, Y., Couzigné, E., Donnio, B., Avérous, L., 2014. Synthesis, structure and properties of fully biobased thermoplastic polyurethanes, obtained from a diisocyanate based on modified dimer fatty acids, and different renewable diols. Eur. Polym. J. 61, 197–205. https://doi.org/10.1016/j.eurpolymj.2014.10.012.

Chen, J., Pascault, J., Taha, M., 1996. Synthesis of polyurethane acrylate oligomers based on polybutadiene polyol. J. Polym. Sci., Part A: Polym. Chem. 34, 2889–2907.

Chladek, G., Kasperski, J., Barszczewska-Rybarek, I., Zmudzki, J., 2013. Sorption, solubility, bond strength and hardness of denture soft lining incorporated with silver nanoparticles. Int. J. Mol. Sci. 14, 563–574. https://doi.org/10.3390/ijms14010563.

Chladek, G., Zmudzki, J., Kasperski, J., 2014. Long-term soft denture lining materials. Mater 7, 5816–5842. https://doi.org/10.3390/ma7085816.

Dębowski, M., Balas, A., 2000. Polyurethane elastomers obtained in polar solvent with N, N′-ethyleneurea as a chain extender. Eur. Polym. J. 36, 601–605. https://doi.org/10.1016/S0014-3057(99)00095-6.

Deng, J., Ren, L., Pan, Y., Gao, H., Meng, X., 2021. Antifungal property of acrylic denture soft liner containing silver nanoparticles synthesized in situ. J. Dent. 106, 103589. https://doi.org/10.1016/j.jdent.2021.103589.

Ge, Q., Jian, B., Li, H., 2022. Shaping soft materials via digital light processing-based 3D printing: a review. Forces Mech. 6, 100074. https://doi.org/10.1016/j.finmec.2022.100074.

Gisselfält, K., Helgee, B., 2003. Effect of soft segment length and chain extender structure on phase separation and morphology in poly (urethane urea) s. Macromol. Mater. Eng. 288, 265–271. https://doi.org/10.1002/mame.200390023.

Goël Brackett, M., Bouillaguet, S., Lockwood, P.E., Rotenberg, S., Lewis, J.B., Messer, R. L.W., Wataha, J.C., 2007. In vitro cytotoxicity of dental composites based on new and traditional polymerization chemistries. J. Biomed. Mater. Res. B Appl. Biomater. 81, 397–402. https://doi.org/10.1002/jbm.b.30676.

Gonzalez, J.B., 1978. Polyurethane elastomers for facial prostheses. J. Prosthet. Dent 39, 179–187.

Hashem, M.I., 2015. Advances in soft denture liners: an update. J. Contemp. Dent. Pract. 16, 314–318. https://doi.org/10.5005/jp-journals-10024-1682.

Šimunović, L., Brenko, L., Marić, A.J., Meštrović, S., Haramina, T., 2025. Rheology of dental photopolymers for SLA/DLP/MSLA 3D printing. Polym 17, 2796. https://doi.org/10.3390/polym17192706.

Inoue, K., Arikawa, H., Fujii, K., Shinohara, N., Kawahata, N., 1985. Viscoelastic properties of oral soft tissue 1. A method of determining elastic modulus of oral soft tissue. Dent. Mater. J. 4, 47–53.

Ishinabe, S., 1991. Mucosal thickness of the denture foundation under occlusal force. Nippon. Hotetsu Shika Gakkai Zasshi 35, 111–124. https://doi.org/10.2186/jjps.35.111.

Isobe, Akio, Sato, Yuji, Kitagawa, Noboru, Shimodaira, Osamu, Hara, Satoshi, et al., 2013. The influence of denture supporting tissue properties on pressure-pain threshold. J. Prosthodontic Res. 57 (4), 275–283. https://doi.org/10.1016/j.jpor.2013.07.002. https://linkinghub.elsevier.com/retrieve/pii/S1883195813000911.

Kamal, M.N.M., 2025. Comparison between relining of ill-fitted maxillary complete denture versus CAD/CAM milling of new one regarding patient satisfaction, denture retention and adaptation. BMC Oral Health 25, 18. https://doi.org/10.1186/s12903-024-05298-z.

Kanie, T., Kadokawa, A., Arikawa, H., Fujii, K., Ban, S., 2005. Mechanical properties of an experimental soft lining material based on urethane oligomer. Dent. Mater. J. 24, 433–439. https://doi.org/10.4012/dmj.24.433.

Kanie, T., Kadokawa, A., Arikawa, H., Fujii, K., Ban, S., 2008. Effects of adding methacrylate monomers on viscosity and mechanical properties of experimental light-curing soft lining materials based on urethane (meth)acrylate oligomers. Dent. Mater. J. 27, 856–861. https://doi.org/10.4012/dmj.27.856.

Kanie, T., Tomita, K., Tokuda, M., Arikawa, H., Fujii, K., Ban, S., 2009. Mechanical properties and cytotoxicity of experimental soft lining materials based on urethane acrylate oligomers. Dent. Mater. J. 28, 501–506. https://doi.org/10.4012/dmj.28.501.

Kasuga, Y., Takahashi, H., Akiba, N., Minakuchi, S., Matsushita, N., Hishimoto, M., 2011. Basic evaluation on physical properties of experimental fluorinated soft lining materials. Dent. Mater. J. 30, 45–51. https://doi.org/10.4012/dmj.2010-084.

Kawano, F., Dootz, E.R., Koran, A., Craig, R.G., 1994b. Sorption and solubility of 12 soft denture liners. J. Prosthet. Dent 72, 393–398. https://doi.org/10.1016/0022-3913(94)90559-2.

Kawano, F., Kon, M., Koran, A., Matsumoto, N., 1994a. Shock-absorbing behavior of four processed soft denture liners. J. Prosthet. Dent 72, 599–605. https://doi.org/10.1016/0022-3913(94)90292-5.

Kitagawa, Y., Yoshida, K., Takase, K., Valanezhad, A., Watanabe, I., Kojio, K., Murata, H., 2020. Evaluation of viscoelastic properties, hardness, and glass transition

temperature of soft denture liners and tissue conditioner. Odontology 108, 366–375. https://doi.org/10.1007/s10266-019-00477-9.
Kowalska, A., Sokolowski, J., Bociong, K., 2021. The photoinitiators used in resin based dental composite—A review and future perspectives. Polym 13, 470. https://doi.org/10.3390/polym13030470.
Kreve, S., Dos Reis, A.C., 2019. Denture liners: a systematic review relative to adhesion and mechanical properties. Sci. World J. https://doi.org/10.1155/2019/6913080.
Lacoste-Ferré, M.H., Demont, P., Dandurand, J., Dantras, E., Duran, D., Lacabanne, C., 2011. Dynamic mechanical properties of oral mucosa: Comparison with polymeric soft denture liners. J. Mech. Behav. Biomed. Mater. 4, 269–274. https://doi.org/10.1016/j.jmbbm.2010.10.005.
Lee, D.-J., Choi, J.Y., Do Kim, H., 1999. Preparation and properties of UV-curable polyurethane acrylate (II)-effect of types and concentration of reactive diluents. J Korean Fiber Society 36, 798–805.
Li, M., Du, M., Wang, F., Xue, B., Zhang, C., Fang, H., 2020. Study on the mechanical properties of polyurethane (PU) grouting material of different geometric sizes under uniaxial compression. Constr. Build. Mater. 259, 119797. https://doi.org/10.1016/j.conbuildmat.2020.119797.
Lytle, R.B., 1962. Soft tissue displacement beneath removable partial and complete dentures. J. Prosthet. Dent 12, 34–43.
Maurya, S.D., Kurmvanshi, S.K., Mohanty, S., Nayak, S.K., 2018. A review on acrylate-terminated urethane oligomers and polymers: synthesis and applications. Polym. Plast. Technol. Eng. 57, 625–656. https://doi.org/10.1080/03602559.2017.1332764.
Meereis, C.T.W., Leal, F.B., Lima, G.S., De Carvalho, R.V., Piva, E., Ogliari, F.A., 2014. BAPO as an alternative photoinitiator for the radical polymerization of dental resins. Dent. Mater. 30, 945–953. https://doi.org/10.1016/j.dental.2014.05.020.
Mishra, S., Chaturvedi, S., Ali, M., Pandey, K.K., Alqahtani, N.M., Alfarsi, M.A., Addas, M.K., Vaddamanu, S.K., Al Ahmari, N.M., Alqahtani, S.M., Yaqoob, A., Alqahtani, W.M.S., 2023. Dimensional stability of light-activated urethane dimethacrylate denture base resins. Polym 15, 744. https://doi.org/10.3390/polym15030744.
Mitra, A., Choudhary, S., Garg, H., Hg, J., 2014. Maxillofacial prosthetic materials-an inclination towards silicones. J. Clin. Diagn. Res. 8, 8–13. https://doi.org/10.7860/JCDR/2014/9229.5244.
Murata, H., Hamada, T., Sadamori, S., 2008. Relationship between viscoelastic properties of soft denture liners and clinical efficacy. Jpn. Dent. Sci. Rev. 44, 128–132. https://doi.org/10.1016/j.jdsr.2008.06.001.
Nakazato, S., Amari, T., Yamaoka, T., 1989. Mechanical properties of UV-cured urethane films. J. Appl. Polym. Sci. 38, 627–643. https://doi.org/10.1002/app.1989.070380404.
Niedźwiedź, M.J., Demirci, G., Kantor-Malujdy, N., El Fray, M., 2023. Influence of photoinitiator type and curing conditions on the photocuring of soft polymer network. Mater 16, 2348. https://doi.org/10.3390/ma16237348.
Onuma, H., Inokoshi, M., Hirayama, D., Inoue, M., Minakuchi, S., 2021. Stress distribution analysis of oral mucosa under soft denture liners using smoothed particle hydrodynamics method. J. Mech. Behav. Biomed. Mater. 117, 104390. https://doi.org/10.1016/j.jmbbm.2021.104390.
Piedra-Cascón, W., Krishnamurthy, V.R., Att, W., Revilla-León, M., 2021. 3D printing parameters, supporting structures, slicing, and post-processing procedures of vat-polymerization additive manufacturing technologies: a narrative review. J. Dent. 109, 103630. https://doi.org/10.1016/j.jdent.2021.103630.
Rokaya, D., Srimaneepong, V., Sapkota, J., Qin, J., Siraleartmukul, K., Siriwongrungson, V., 2018. Polymeric materials and films in dentistry: an overview. J. Adv. Res. 14, 25–34. https://doi.org/10.1016/j.jare.2018.05.001.
Santawisuk, W., Kanchanavasita, W., Sirisinha, C., Harnirattisai, C., 2013. Mechanical properties of experimental silicone soft lining materials. Dent. Mater. J. 32, 970–975. https://doi.org/10.4012/dmj.2013-083.
Sato, Y., Abe, Y., Okane, H., Tsuga, K., 2000. Finite element analysis of stress relaxation in soft denture liner. J. Oral Rehabil. 27, 660–663. https://doi.org/10.1046/j.1365-2842.2000.00566.x.
Schwarz, D., Pagáč, M., Petruš, J., Polzer, S., 2022. Effect of water-induced and physical aging on mechanical properties of 3D printed elastomeric polyurethane. Polym 14, 5496. https://doi.org/10.3390/polym14245496.
Shiga, H., Terada, Y., Ikebe, K., Akagawa, Y., Hirai, T., Inoue, H., 2007. Guideline for denture relining. Prosthodont. research & practice, 6, 209–216. https://doi.org/10.2186/prp.6.209.
Sigusch, B.W., Völpel, A., Braun, I., Uhl, A., Jandt, K.D., 2007. Influence of different light curing units on the cytotoxicity of various dental composites. Dent. Mater. 23, 1342–1348. https://doi.org/10.1016/j.dental.2006.11.013.
Songsang, N., Anunmana, C., Pudla, M., Eiampongpaiboon, T., 2022. Effects of Litsea cubeba essential oil incorporated into denture soft lining materials. Polym 14, 3261. https://doi.org/10.3390/polym14163261.
Szycher, M., 2012. Szycher's Handbook of Polyurethanes, second ed. CRC press, Boca Raton.
Tallgren, A., 2003. The continuing reduction of the residual alveolar ridges in complete denture wearers: a mixed-longitudinal study covering 25 years. J. Prosthet. Dent 89, 427–435. https://doi.org/10.1016/0022-3913(72)90188-6.
Tanaka, S., 1973. A study on creep of oral mucousa. J. Jpn. Prosthodont. Soc. 14, 358–378.
Tanimoto, Y., Saeki, H., Kimoto, S., Nishiwaki, T., Nishiyama, N., 2009. Evaluation of adhesive properties of three resilient denture liners by the modified peel test method. Acta Biomater. 5, 764–769. https://doi.org/10.1016/j.actbio.2008.08.021.
Tasic, S., Bozic, B., Dunjic, B., 2004. Synthesis of new hyperbranched urethane-acrylates and their evaluation in UV-curable coatings. Prog. Org. Coating 51, 320–327. https://doi.org/10.1016/j.porgcoat.2004.07.021.
Tzeng, J.J., Yang, T.S., Lee, W.F., Chen, H., Chang, H.M., 2021. Mechanical properties and biocompatibility of urethane acrylate-based 3D-Printed denture base resin. Polym 13, 82. https://doi.org/10.3390/polym.
Van Krevelen, D.W., te Nijenhuis, K., 2009. Properties of Polymers: Correlations with Chemical Structure, fourth ed. Elsevier, Amsterdam.
Wienen, D., Gries, T., Cooper, S.L., Heath, D.E., 2023. An overview of polyurethane biomaterials and their use in drug delivery. J. Contr. Release 363, 376–388. https://doi.org/10.1016/j.jconrel.2023.09.036.
Xu, X., He, L., Zhu, B., Li, Jiyao, Li, Jianshu, 2017. Advances in polymeric materials for dental applications. Polym. Chem. 8, 807–823. https://doi.org/10.1039/c6py01957a.
Yamaga, Y., Kanatani, M., Nomura, S., 2015. Usefulness of a rotation-revolution mixer for mixing powder-liquid reline material. J. Prosthodont. Res. 59, 71–78. https://doi.org/10.1016/j.jpor.2014.11.002.
Yoo, H.J., Lee, Y.H., Kwon, J.Y., Kim, H.-D., 2001. Comparision of the properties of UV-cured polyurethane acrylates containing different diisocyanates and low molecular weight diols. Fibers Polym. 2, 122–128. https://doi.org/10.1007/BF02875324.
Zhou, R., Gao, W., Xia, L., Wu, H., Guo, S., 2018. The study of damping property and mechanism of thermoplastic polyurethane/phenolic resin through a combined experiment and molecular dynamics simulation. J. Mater. Sci. 53, 9350–9362. https://doi.org/10.1007/s10853-018-2218-3.
Zhu, G., Hou, Y., Xu, J., Zhao, N., 2022. Digital light processing 3D printing of enhanced polymers via interlayer welding. Macromol. Rapid Commun. 43. https://doi.org/10.1002/marc.202200053.